Urban Climate 56 (2024) 102038

Contents lists available at ScienceDirect

Urban Climate

journal homepage: www.elsevier.com/locate/uclim

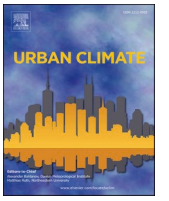

# Statistical and modeling analyses of urban impacts on winter precipitation

Jiahui Liu [a], Yue Xing [a], Dan Li [b], Long Yang [c], Guangheng Ni [a,*]

[a] State Key Laboratory of Hydroscience and Engineering and Department of Hydraulic Engineering, Tsinghua University, Beijing, China
[b] Department of Earth and Environment, Boston University, Boston, USA
[c] School of Geography and Ocean Science, Nanjing University, Nanjing, China

ARTICLE INFO

*Keywords:*
Statistical analyses
WRF
Urban impact
Winter precipitation
Snowfall

ABSTRACT

Despite the implications of winter precipitation for socioeconomic activities and transportation services, the influence of cities on winter precipitation is less studied compared to that on summer precipitation. Here we investigated the statistical relations between precipitation, temperature, and impervious surface fraction in 12 major cities across the contiguous United States. The results showed negative correlations between snowfall intensity and impervious surface fraction. The correlations depend on latitude and the distance to complex terrain features (water bodies or topography), with stronger correlations for inland cities than coastal/lakeside cities. We further selected Kansas City for modeling analyses based on the Weather Research and Forecasting model. Simulation results indicated that the heating effect of urban land occurs in the near-surface atmosphere during the precipitation period, leading to changes of different hydrometeors and an overall tendency of reducing snowfall but increasing rainfall.

## 1. Introduction

Urban impacts on precipitation have received considerable attention since the pioneering Metropolitan Meteorological Experiment (METROMEX) in the 1970s (Changnon Jr et al., 1971; Changnon Jr, 1975). This evolves into a pressing issue as urban population witnesses rocketing increases around the globe (Grimm et al., 2008) and cities are suffering from multiple precipitation-related environmental hazards such as flooding, droughts, and snow storms (WBGU, 2016). Compared to surrounding rural areas, cities are characterized with higher surface and near-surface air temperatures, taller roughness elements, and severe air pollution (Oke et al., 2017). These attributes modify the spatial and temporal variability of precipitation.

Empirical and modeling analyses reveal three main mechanisms through which cities affect precipitation (mostly rainfall, Shepherd, 2005, 2013; Liu and Niyogi, 2019; Pielke et al., 2007, 2011; Li et al., 2013). These three mechanisms are the urban heat island effect, the urban canopy effect, and elevated airborne aerosols. The urban heat island effect refers to the fact that urban areas typically have higher temperatures than their surrounding rural areas. The urban heat island effect contributes to more unstable atmospheric conditions in urban areas, leading to development of localized convection or rising air parcels, which then cool, condense, and form clouds and potentially precipitation (Bornstein and Lin, 2000; Dixon and Mote, 2003; Yang et al., 2014a; Miao et al., 2009; Niyogi et al., 2006; Kim et al., 2021; Shu et al., 2023). The urban canopy effect refers to that buildings, roads, and other urban canopy characteristics can alter wind patterns and thus the transfer of heat and moisture in the lower atmosphere, leading to convergence of

* Corresponding author.
*E-mail address:* ghni@tsinghua.edu.cn (G. Ni).

https://doi.org/10.1016/j.uclim.2024.102038
Received 18 April 2023; Received in revised form 18 October 2023; Accepted 22 June 2024
Available online 9 July 2024
2212-0955/© 2024 Elsevier B.V. All rights are reserved, including those for text and data mining, AI training, and similar technologies.

air masses near the city. This convergence further results in upward motion of air and, subsequently, cloud formation and precipitation (Niyogi et al., 2006; Yang et al., 2021; Zhang et al., 2018; Dou et al., 2015; Bornstein and LeRoy, 1990). Elevated airborne aerosols can act as cloud condensation nuclei and affect cloud microphysics. They may enhance cloud droplet formation and influence precipitation patterns (Rosenfeld, 2000; Zhong et al., 2017; Taichen et al., 2023). However, urban-induced precipitation anomalies demonstrate diverse signatures (e.g., the preferential distribution of rainfall enhancement, see Liu and Niyogi (2019) for a review). For instance, Yang et al. (2019) examined two back-to-back thunderstorms over Phoenix, Arizona. Their results showed that interactions of urban-induced circulation with an outflow boundary propagating from the surrounding mountains led to enhanced rainfall for the first storm episode, while the urban heat island effect was responsible for increased rainfall over the downtown region for the second storm episode. In addition, the role of land-water boundaries (i.e., through land-sea/lake breeze) in urban rainfall anomalies has been emphasized in previous studies over the Milwaukee–Lake Michigan region (e.g. Yang et al., 2014b) and the Baltimore-Washington region (e.g. Ryu et al., 2016). These studies highlighted the importance of interactions between complex terrain (i.e., topography, land-water boundaries) and cities in affecting the spatiotemporal variability of rainfall.

Compared to warm-season rainfall, urban impacts on winter precipitation (i.e., snowfall or mixture of snow and rainfall) are relatively less examined. The urban heat island effect shows strong seasonality (Zhou et al., 2016; Gabriele et al., 2020). Some studies found that the urban heat island effect is stronger during winter months than summer months (Kim and Baik, 2005; Hinkel and Nelson, 2007; Ramamurthy and Sangobanwo, 2016; Miles and Esau, 2017; Yang and Bou-Zeid, 2018), suggesting that urban-induced winter precipitation anomalies could be even more notable (Montávez et al., 2000; Li et al., 2016). Based on empirical analyses of 40-year in-situ observations from 14 weather stations, Wang et al. (2009) showed that both the urban heat island and urban dry island effects led to enhanced evaporation of hydrometeors over Beijing, and thus reduced winter precipitation acccumulation. Similarly, Johnson and Shepherd (2018) reported significant negative correlations between the observed intensity of mixed precipitation and the distance of weather stations to the city center. Modeling analyses further confirmed the role of the urban heat island effect in inducing winter precipitation anomalies (Changnon, 2004; Grillo and Spar, 1971; Jones and Jiusto, 1980; Malevich and Klink, 2011; Thériault et al., 2010; Johnson et al., 2021). For instance, Guo et al. (2019) showed that urban-induced temperature increases in the lower atmosphere intensified the melting processes of snow within the Fifth Ring road of Beijing (i.e., the downtown region) for a snow storm in 2018. Studies also found that increased urban aerosols as cloud condensation nuclei could inhibit snow production and reduce winter precipitation (Bokwa, 2009; Givati and Rosenfeld, 2004; Rosenfeld, 2000). However, existing knowledge is mostly based on isolated case studies. Comparative studies across a large collection of cities, which enable improved characterization of urban-induced winter precipitation anomalies, are still quite limited.

Ample evidence has highlighted the role of large water bodies (e.g., sea or lake) in determining the intensity and distribution of snowfall. When cold air flows over warmer lake surfaces, the water vapor evaporating from the lake condenses when mixed with the cold air, forming snow on the lake or downwind of the lake (Hayhoe et al., 2010; Niziol et al., 1995; Kitagawa et al., 2022). Similar effects were observed along coastal regions (Yang et al., 2009). Moreover, orographic lifting was also found to be important for convective processes and the properties of hydrometeors (e.g., types, size, density) (Notaro et al., 2015). However, the interactions of cities and complex terrain in modulating the spatiotemporal variability of winter precipitation have received less attention.

In this study, we aim to improve our understanding of how urban land affects winter precipitation using statistical and modeling analyses. The statistical analyses were performed over 12 major cities across the contiguous United States. These cities demonstrated a spectrum of phsyiographic attributes, including latitude, topography, and land-water boundaries. We further selected Kansas City for modeling analyses based on the Weather Research and Forecasting (WRF) model, which has been widely used to study urban impacts on precipitation (Feili et al., 2023; Donmez et al., 2022; Sati and Mohan, 2021; Doan et al., 2022; Louis et al., 2020; Doan et al., 2023). We selected Kansas City because it is an inland city located in the Central Great Plains with little topographic relief and far away from major water bodies. The numerical simulations over Kansas City were expected to highlight the impact of cities on winter precipitation.

The rest of the paper is organized as follows. Section 2 describes data and methodology, including observations and the setup of numerical experiments. Results are provided in section 3, followed by a summary and conclusions in section 4.

## 2. Data and methodology

### 2.1. Statistical analyses

We investigated the statistical relations between various land surface parameters (especially impervious surface fraction) and meteorological variables (temperature and precipitation) using observational data collected by weather stations. Such statistical analyses were conducted for the period of 2009–2018 in 12 cities over the contiguous United States. These cities were selected using the following steps.

First, the 50 largest cities in terms of population were chosen. For each city, we defined a circular buffer with a radius of 150 km to collect weather station data. When the buffers of different cities overlapped, data from the same weather station might be selected by different cities. To avoid such scenarios, only the city with the largest population was retained when the buffers of different cities overlapped, which resulted in 37 cities with the distance between each other greater than 150 km. The buffer size of 150 km was a rough estimate of the footprint size of a city. It was chosen as a compromise between being reasonable (e.g., the buffer size should not be too large) and ensuring that each city has enough stations for analysis (namely, the buffer size cannot be too small).

Second, for these 37 cities we collected weather station data (snowfall, rainfall and temperatures) from the Daily Global Historical Climatology Network (Menne et al., 2012) within the buffer size of 150 km. To study the correlations between precipitation (snowfall and rainfall) and temperatures as well as the correlations between land surface parameters and meteorological variables (precipitation

and temperatures), we required four meteorological variables (daily maximum temperature, daily minimum temperature, daily snowfall and daily rainfall amounts) to be simultaneously available. If any of the four variables was missing on a day, then all four variables were treated as missing for that day. Afterwards, we tested different thresholds of missing data for determining whether a station was kept for analysis or discarded. With 60% as the threshold (namely, if a station had more than 40% of data missing, then it was discarded), 868 stations remained. With 90% as the threshold, 394 stations remained.

Third, we required each city to have more than 30 stations. With 60% as the threshold, 12 cities remained. These 12 cities included 4 coastal cities, 4 lakeside cities and 4 inland cities based on the criteria to be discussed shortly. If the threshold was set to 70%, 9 cities would have remained, with only 2 coastal cities. As a compromise, we used 60% as the threshold and were left with 12 cities. We also tested 50% as the threshold and our key findings were not altered.

As just alluded to, we classified cities into inland cities, coastal cities, and lakeside cities. Following previous studies on the relationship between precipitation and the distance to coastline (Makarieva et al., 2009; Ogino et al., 2016), the coastal region was defined as any area within 300 km from the coastline. Hence cities within 300 km from the coastline were defined as coastal cities. Similarly, cities close to the Great Lakes (< 300 km) were defined as lakeside cities. The remaining cities were defined as inland cities. According to this classification, there were 4 coastal cities, 4 lakeside cities and 4 inland cities (see Fig. 1).

In this study, January, February, March, November and December were treated as the winter season, which covers most of the snowfall events over the 12 cities we selected. Days with snowfall greater than zero were treated as snowfall days for each station. Snowfall and temperature data on snowfall days were used to analyze the correlation between snowfall and other variables. Similarly, the data on rainfall days were used to analyze the correlation between rainfall and other variables. It is worth noting that during the winter period, snowfall and rainfall often occurred at the same time, that is, mixed precipitation occurred. The 10-year (2009–2018) winter mean values of precipitation and temperatures on snowfall days and rainfall days were first calculated for each station. For each city, the 10-year winter mean values of precipitation and temperature across all stations were then spatially averaged. The spatial averages were taken as the reference and the difference between the value of each station and the reference (namely, the spatial anomaly) was used for analysis.

Using these spatial anomalies, we analyzed the linear correlation between precipitation (both snowfall and rainfall) and temperatures based on the following equations:

$$S = \alpha_1' + \beta_1' T_{max}, \tag{1}$$

$$S = \alpha_2' + \beta_2' T_{min}, \tag{2}$$

$$R = \alpha_3' + \beta_3' T_{max}, \tag{3}$$

$$R = \alpha_4' + \beta_4' T_{min}, \tag{4}$$

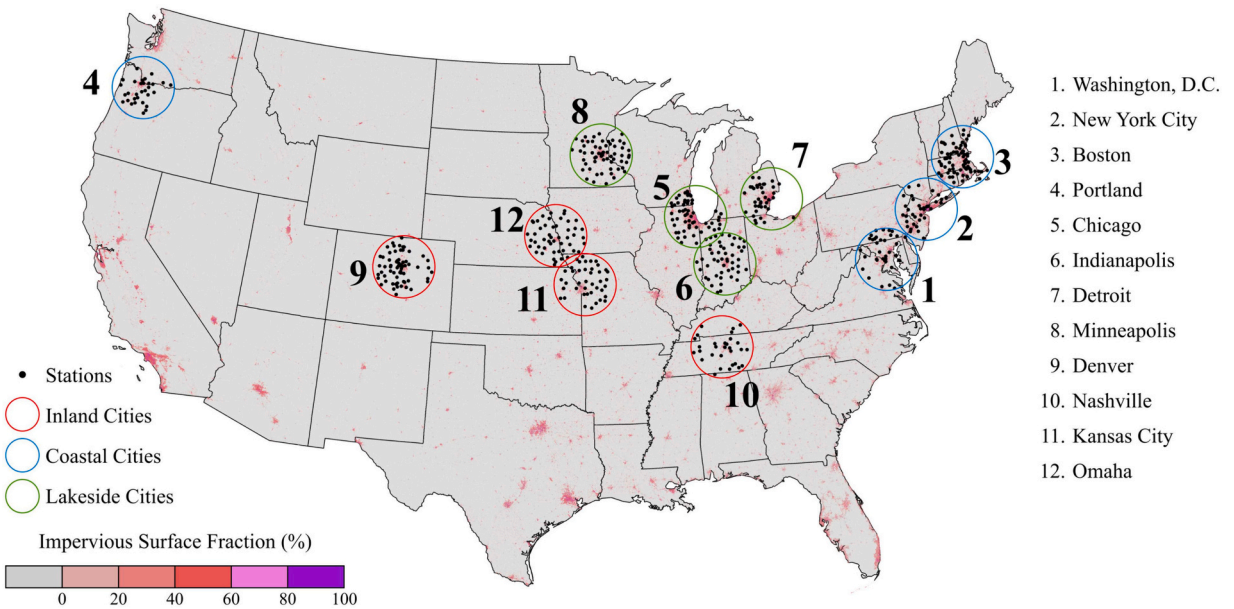


**Fig. 1.** The locations of selected U.S. cities. The impervious surface fraction (%) from the National Land Cover Database (NLCD) 2011 Percent Developed Imperviousness is shown by colour. Red circles represent inland cities, green circles represent lakeside cities, and blue circles represent coastal cities. Black dots represent valid stations. (For interpretation of the references to colour in this figure legend, the reader is referred to the web version of this article.)

where $S$ is the mean daily snowfall on snowfall days, $R$ is the mean daily rainfall on rainfall days. $T_{max}$ and $T_{min}$ (in $^{\circ}C$) are the corresponding mean daily maximum and minimum temperature, respectively. The $\alpha'$ and $\beta'$ are regression coefficients. We expected that snowfall was negatively correlated with temperatures (i.e., negative values of $\beta_1'$ and $\beta_2'$) and rainfall was positively correlated with temperatures (i.e., positive values of $\beta_3'$ and $\beta_4'$).

Furthermore, multiple linear regression was performed based on the following equation to isolate the effect of various land surface parameters:

$$S = \alpha_1 + \beta_{11} Imp + \beta_{12} Dis + \beta_{13} Lat, \tag{5}$$

where *Imp* is the impervious surface fraction (in %), *Dis* is the distance from water bodies (in *km*, only for coastal cities and lakeside cities), Lat is the latitude (degree), $\alpha$ and $\beta$ are regression coefficients. The same analysis were performed for $T_{max}$ and $T_{min}$:

$$T_{max} = \alpha_2 + \beta_{21} Imp + \beta_{22} Dis + \beta_{23} Lat, \tag{6}$$

$$T_{min} = \alpha_3 + \beta_{31} Imp + \beta_{32} Dis + \beta_{33} Lat. \tag{7}$$

The impervious surface fraction (*Imp*) was from the National Land Cover Database (NLCD) 2011 Percent Developed Imperviousness. Following previous work (Foissard et al., 2019; Suomi et al., 2012; Zhao et al., 2011; Pauleit et al., 2005; Eliasson and Svensson, 2003), a circular buffer with a radius of 500 m was established for each station and the mean value of impervious surface fraction (%) within the buffer was computed as *Imp*. We conducted analysis with different buffer sizes and found that our findings were not altered as long as the buffer size was in a reasonable range (200–1000 m). A higher impervious surface fraction (%), which indicates a larger proportion of built-up area surrounding the station, was assumed to represent a higher urbanization level. We note that besides the impervious surface fraction, there are numerous urban characteristics factors that can influence atmospheric variables. In this study, we chose the impervious surface fraction as a bulk parameter that reflects the degree of urbanization. However, it is important to acknowledge that this assumption has its limitations. The distance from the coastline was defined as the shortest distance from a station to the coastline for coastal cities and the shoreline for lakeside cities.

### 2.2. Numerical simulations

The statistical analyses were complemented by numerical modeling analyses. Since it is impossible to conduct simulations for all winter precipitation events during the research period over all cities, as a logical starting point we selected one city, which is Kansas City. The reason that we selected Kansas City is because our statistical analyses (to be presented in Section 3.1) revealed that winter precipitation is influenced by various factors, including impervious surface fraction, topography, and distance from waterbodies. Since Kansas City is located in the Central Great Plains, with little topographic relief (Fig. 2b) and far away from any major water bodies, numerical simulations over Kansas City will highlight the impact of cities on winter precipitation. Kansas City is a medium size city in the United States. The population of Kansas City is estimated to be over 0.5 million people, while the metropolitan area includes over 2 million people. The city is around 319 mile$^2$, while the entire metropolitan area is much larger, around 7900 mile$^2$. The city's building

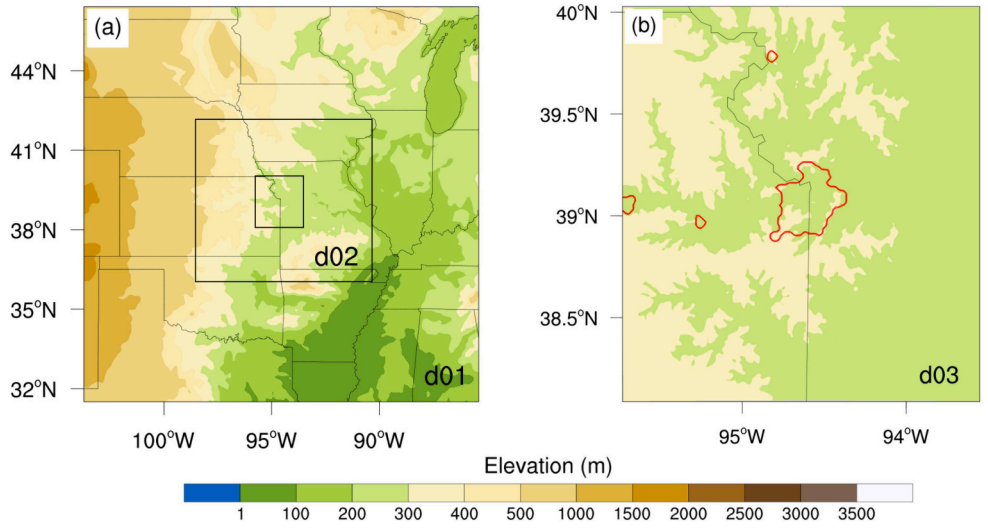


**Fig. 2.** (a) Three nested domains used for WRF simulations with elevation in colour over. (b) The spatial extent of domain 3 with elevation in colour. The red polygon represents the urban boundary by encircling the urban land use type. (For interpretation of the references to colour in this figure legend, the reader is referred to the web version of this article.)

morphology is marked by a mix of high-rise buildings in the central business district, mid-rise structures, and residential suburbs.

Three different types of winter precipitation over Kansas City were simulated to investigate how urbanization impacts the spatiotemporal characteristics of different types of winter precipitation. Furthermore, a season-long simulation over Kansas City (referred to as the season-long simulation) was conducted to demonstrate that the findings from individual events were generalizable, at least over Kansas City.

To perform numerical simulations, the WRF model was used (Skamarock et al., 2008). Specifically, the Advanced Research WRF (ARW) version 3.7 was adopted in this study. Three two-way nested domains were used as the basic configuration. There were 200 × 200, 220 × 220 and 187 × 211 grid cells, with the corresponding resolutions of 9 km, 3 km, and 1 km, respectively (Fig. 2). There were 1086 grid cells designated as urban in domain 3, accounting for about 3%. The model contained 54 sigma levels in the vertical direction, with the model top set at 50 hPa. The time step for the outermost domain was 15 s. The initial and boundary conditions were provided by the National Center for Environmental Prediction (NCEP) Global Final Analysis (FNL) fields (https://rda.ucar.edu/datasets/ds083.2/), with a spatial resolution of 1 degree and a temporal resolution of 6 h. The MODIS land use dataset provided by WRF was used to represent land use and land cover over the study region.

The other key physics options for the WRF model were listed in Table 1. WSM6 was chosen as the microphysical parametrization (Hong et al., 2006). The radiation schemes included the Dudhia shortwave radiation scheme (Dudhia, 1989) and the Rapid Radiative Transfer Model (RRTM) longwave radiation scheme (Mlawer et al., 1997). The selected planetary boundary layer (PBL) scheme was MYJ (Janjić, 1994). The Noah land surface model (Chen and Dudhia, 2001) and Monin-Obukhov Surface Layer scheme (Monin and Obukhov, 1954) were applied for parameterizing surface processes. Cumulus scheme was turned off for all domains because the largest horizontal grid was less than 10 km (Stensrud, 2007). The single-layer Urban Canopy Model (UCM) (Chen et al., 2011) was used to capture urban characteristics. The single-layer UCM model represents cities as street canyons composed of homogeneous buildings and streets. Although it lacks vertical atmospheric variations and terrain features, the single-layer UCM was widely employed in urban simulations. Anthropogenic heat flux was set to 90 $Wm^{-2}$, the highest value of default settings. Table 1 provided a summary of all key physics schemes used in WRF simulations of this study. The same model configuration was used for all simulations. National snowfall analysis data (https://www.nohrsc.noaa.gov/snowfall/) and the Integrated Multi-satellitE Retrievals for GPM (IMERG) Final Precipitation data (https://disc.gsfc.nasa.gov/datasets/GPM_3IMERGDF_06/summary) were used to evaluate the model performance. National snowfall analysis data is 24-h accumulated, with a spatial resolution of 0.04 degree. IMERG data is also 24-h accumulated, with a spatial resolution of 0.1 degree.

For all simulations, two scenarios were set up to assess the effects of urban land. The control (CTRL) scenario (Fig. 3a) represented the MODIS land use conditions over this region. For the No-Urban (NU) scenario (Fig. 3b), cities were removed by replacing the urban land with the dominant rural land cover type in the surrounding.

For each event, a two-day period was studied. For the snow only event (Kansas City - Snow), the simulation period was from 1800 LT 03–1800 LT 05 February 2014 (LT: Local Time). For the rain only event (Kansas City - Rain), the simulation period was from 1800 LT 08–1800 LT 10 March 2010. For the mixed precipitation event (Kansas City - Mix), the simulation period was from 1800 LT 04–1800 LT 06 February 2010. The synoptic conditions for these three events were shown in Fig. 5 in Section 3b. Precipitation from these three events were primarily large-scale precipitation instead of convective precpitation based on ERA5 reanalysis data (Hersbach et al., 2018). For the season-long simulation, the simulation period was from 1800 LT 30 October 2009–1800 LT 01 April 2010. The results from domain 3 were analyzed due to the high spatial resolution of domain 3 unless noted otherwise.

## 3. Results

### 3.1. Statistical analyses

#### 3.1.1. The relation between precipitation and temperature

First, we examined the relations between precipitation (snowfall and rainfall) and temperatures ($T_{max}$ and $T_{min}$). The fitted values of $\beta'$ based on the Eqs.1–4 were summarized in Table 2. The results indicated that in general snowfall was negatively correlated with temperatures ($\beta'_1 < 0$, $\beta'_2 < 0$), while rainfall was positively correlated with temperatures ($\beta'_3 > 0$, $\beta'_4 > 0$), as expected. This is also demonstrated in Fig. 4, which presents the results for Kansas City. While these results were consistent with physical intuition, precipitation and temperatures were not only affected by the impervious surface fraction but also other factors such as the distance from

**Table 1**
Overview of the WRF physics options.

| Physics | Scheme | Reference |
|---|---|---|
| Microphysics | WSM6 | Hong and Lim (2006) |
| PBL | MYJ | Janjić (1994) |
| Shortwave radiation | Dudhia | Dudhia (1989) |
| Longwave radiation | RRTM | Mlawer et al. (1997) |
| Land surface scheme | Noah LSM | Chen and Dudhia (2001) |
| Surface layer scheme | Monin-Obukhov | Monin and Obukhov (1954) |
| Cumulus | None | None |
| Surface urban physics | UCM | Chen et al. (2011) |

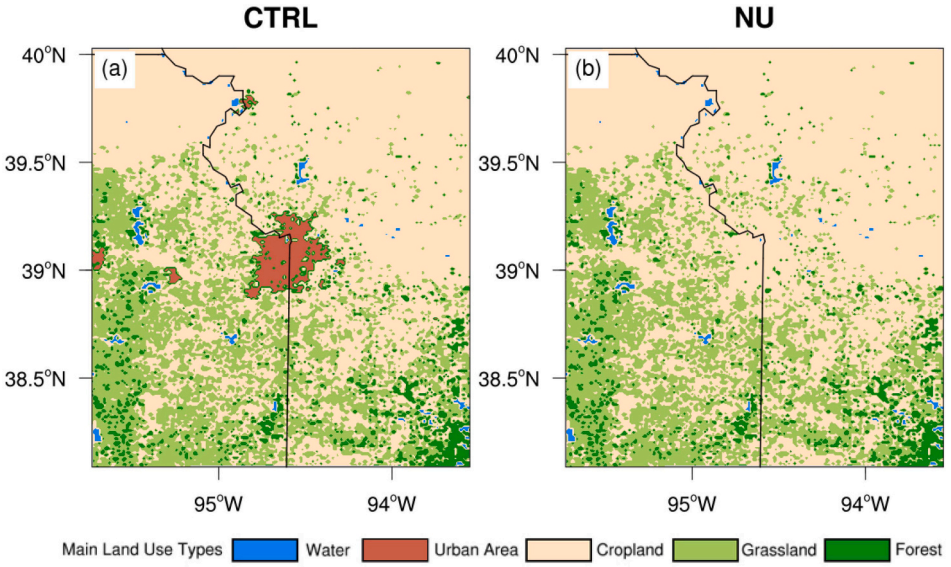


**Fig. 3.** Land use and land cover of domain 3 for CTRL (top) and NU (bottom) scenarios over Kansas City.

**Table 2**
The fitted values of $\beta'$ in Eqs. 1–4. Coefficients are statistically significantly different from zero at the level of 0.05 (*) and 0.1 (#).

| | | $S$ | | $R$ | |
|---|---|---|---|---|---|
| | | $T_{max}$ | $T_{min}$ | $T_{max}$ | $T_{min}$ |
| | | $\beta_1'$ | $\beta_2'$ | $\beta_3'$ | $\beta_4'$ |
| Coastal | New York City | 2.9092 | 1.9594 | 0.2542* | 0.1822* |
| | Washington, D.C. | − 1.4641 | − 3.438* | 0.0825 | 0.0614# |
| | Boston | − 2.1293 | − 1.0508 | 0.4177* | 0.341* |
| | Portland | − 10.9371* | − 3.412 | − 0.4384 | − 0.2252 |
| Lakeside | Chicago | − 1.6642 | − 1.1925 | 0.3185* | 0.2033* |
| | Indianapolis | − 0.7548 | − 0.3185 | 0.5788* | 0.5669* |
| | Detroit | − 3.002* | − 0.6513 | 0.5257* | 0.3743* |
| | Minneapolis | − 0.9142 | − 1.9061# | 0.2693# | 0.0831 |
| Inland | Denver | − 0.9695 | − 0.8913 | 0.0277 | 0.064 |
| | Nashville | − 5.023# | − 4.2965 | 0.2209 | 0.4625* |
| | Kansas City | − 6.9128* | 5.9687* | 0.552* | 0.6162* |
| | Omaha | − 2.5475* | − 3.1221* | 0.281* | 0.2746* |

coast, latitude, and topography. To isolate the impact of these various land surface parameters, we used Eqs.5–7.

*3.1.2. The relation between precipitation/temperature and impervious surface fraction compounded by other factors*

The fitted values of $\beta$ based on the Eqs.5–7 were summarized in Table 3. For all 12 cities, snowfall and impervious surface fraction were negatively correlated (with $\beta_{11} < 0$). This suggested that snowfall decreased with increasing impervious surface fraction. The negative correlation between snowfall and impervious surface fraction was generally more significant for inland cities than other cities.

For coastal cities, snowfall was more affected by the distance from the coastline (the correlation coefficient $\beta_{12}$ was significant). However, the correlation coefficient showed different signs for different cities. More specifically, for New York City and Boston, the correlation coefficient $\beta_{12}$ was negative, while for the other coastal cities, the correlation coefficient $\beta_{12}$ was positive. The different signs suggested that the influence of ocean on snowfall may be opposite under different conditions. On the one hand, when the cold air from the land meets up mith the warm, moist air from the ocean, snow might form. For example, Nor'easters, which are major snowfall-producing cyclones in the Northeastern United States, mainly move along the coastline and produce snow during the winter period. So for cities in this region like New York City and Boston, snowfall might form as water vapor from the ocean meets the cold air from the land, leading to the negative correlation between snowfall and the distance from the coast. On the other hand, due to the large heat capacity of water, temperatures near the ocean are often higher in winter. Namely, temperatures are negatively related to the distance from the coastline, as can be seen from the values of $\beta_{22}$ and $\beta_{32}$ in Table 3. Higher temperatures may cause the melting of snowfall, leading to less snowfall. These contrasting effects might be the reason why the correlation between snowfall and the distance

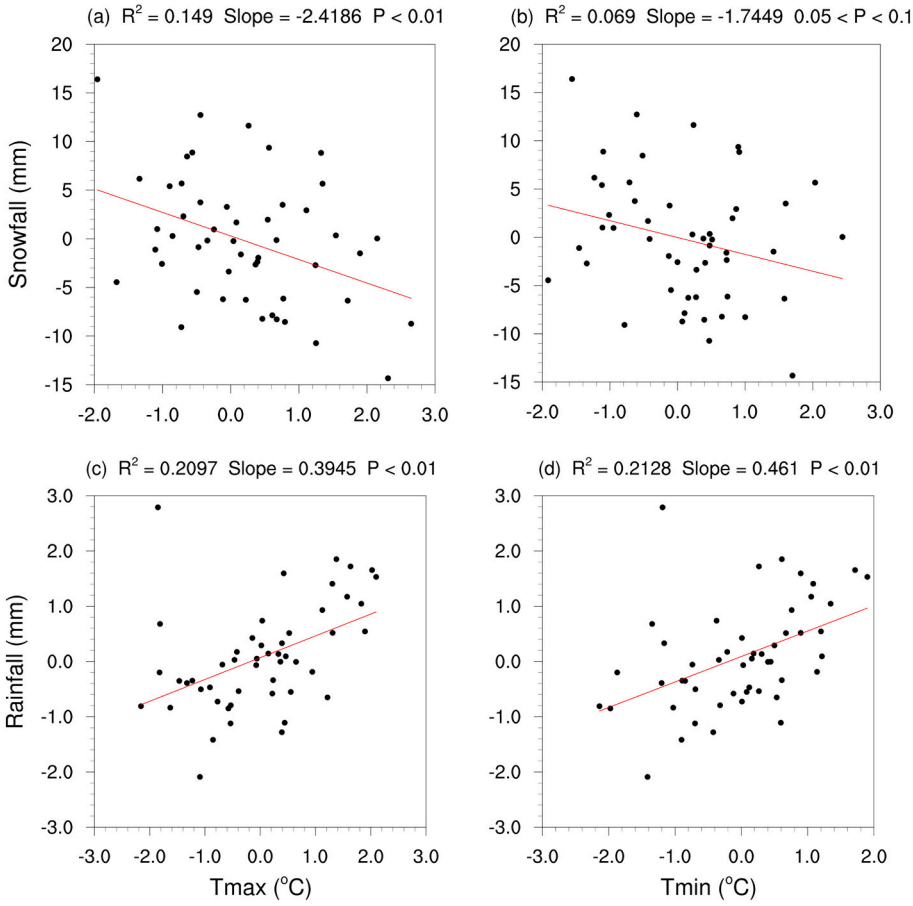


**Fig. 4.** The unary linear regression results between independent variables (Snowfall and Rainfall) and dependent variables (Tmax and Tmin) in Kansas City.

**Table 3**
The fitted values of $\beta$ in Eqs. 5–7. Coefficients are statistically significantly different from zero at the level of 0.01 (*) and 0.1 (#).

| | | $S$ | | | $T_{max}$ | | | $T_{min}$ | | |
|---|---|---|---|---|---|---|---|---|---|---|
| | | *Imp* | *Dis* | *Lat* | *Imp* | *Dis* | *Lat* | *Imp* | *Dis* | *Lat* |
| | | $\beta_{11}$ | $\beta_{12}$ | $\beta_{13}$ | $\beta_{21}$ | $\beta_{22}$ | $\beta_{23}$ | $\beta_{31}$ | $\beta_{32}$ | $\beta_{33}$ |
| Coastal | New York City | −0.1617# | −0.1679* | 0.6579 | 0.007 | −0.0125* | −0.6938* | 0.0187# | −0.0274* | −0.2969 |
| | Washington, D. C. | −0.1734 | 0.063# | 1.9781 | 0.006 | −0.0003 | −1.1511* | 0.0196# | −0.0081# | −1.048* |
| | Boston | −0.048 | −0.0941# | 3.3528 | 0.0137* | −0.0096* | −0.8634* | 0.0242* | −0.0167* | −1.0736* |
| | Portland | −0.1251 | 0.1886# | −9.5316 | −0.0077 | −0.0182* | 0.0729 | −0.0009 | −0.009# | 0.2493 |
| Lakeside | Chicago | −0.0157 | 0.0231 | 1.0808 | −0.0015 | −0.0045# | −0.3348# | 0.0236* | −0.0056# | −0.1607 |
| | Indianapolis | −0.00683 | −0.019 | −2.4287 | −0.0058 | −0.0007 | −0.8496# | 0.0212# | 0.0014 | −0.4966 |
| | Detroit | −0.0111 | −0.028 | −0.7669 | 0.0006 | −0.0057 | −0.1342 | 0.0183# | −0.0061 | −0.1964 |
| | Minneapolis | −0.045 | 0.0022 | −1.0324 | −0.0041 | −0.0091* | −1.1366* | 0.0191* | −0.0125* | −1.6144* |
| Inland | Denver | −0.2325# | | 4.0124 | 0.0456* | | −0.3929 | 0.055* | | 0.6044# |
| | Nashville | −0.3612# | | 13.3458* | 0.0231# | | −0.9015* | 0.0318* | | −0.7704* |
| | Kansas City | −0.0595 | | 1.705 | 0.0157 | | −0.4078# | 0.0205# | | −0.3795# |
| | Omaha | −0.1821* | | 1.4756 | 0.008 | | −0.7504* | 0.0194# | | −0.6916* |

from the coastline was not of the same sign across different coastal cities. Unlike coastal cities, the distance to lakes did not present a significant impact on snowfall for lakeside cities.

For temperatures, the negative correlation between daily maximum temperature and latitude ($\beta_{23} < 0$) was often significant, indicating that the highest temperature one station could reach was at least partially determined by the latitude of the station. While daily minimum temperature also tended to be significantly affected by latitude, it was highly correlated with the impervious surface fraction ($\beta_{31} > 0$). The finding that daily maximum temperature was not significantly correlated with impervious surface fraction but daily minimum temperature was significantly correlated with impervious surface fraction is consistent with the traditional paradigm that the urban heat island effect is stronger and more perceptible during nighttime (Oke et al., 2017).

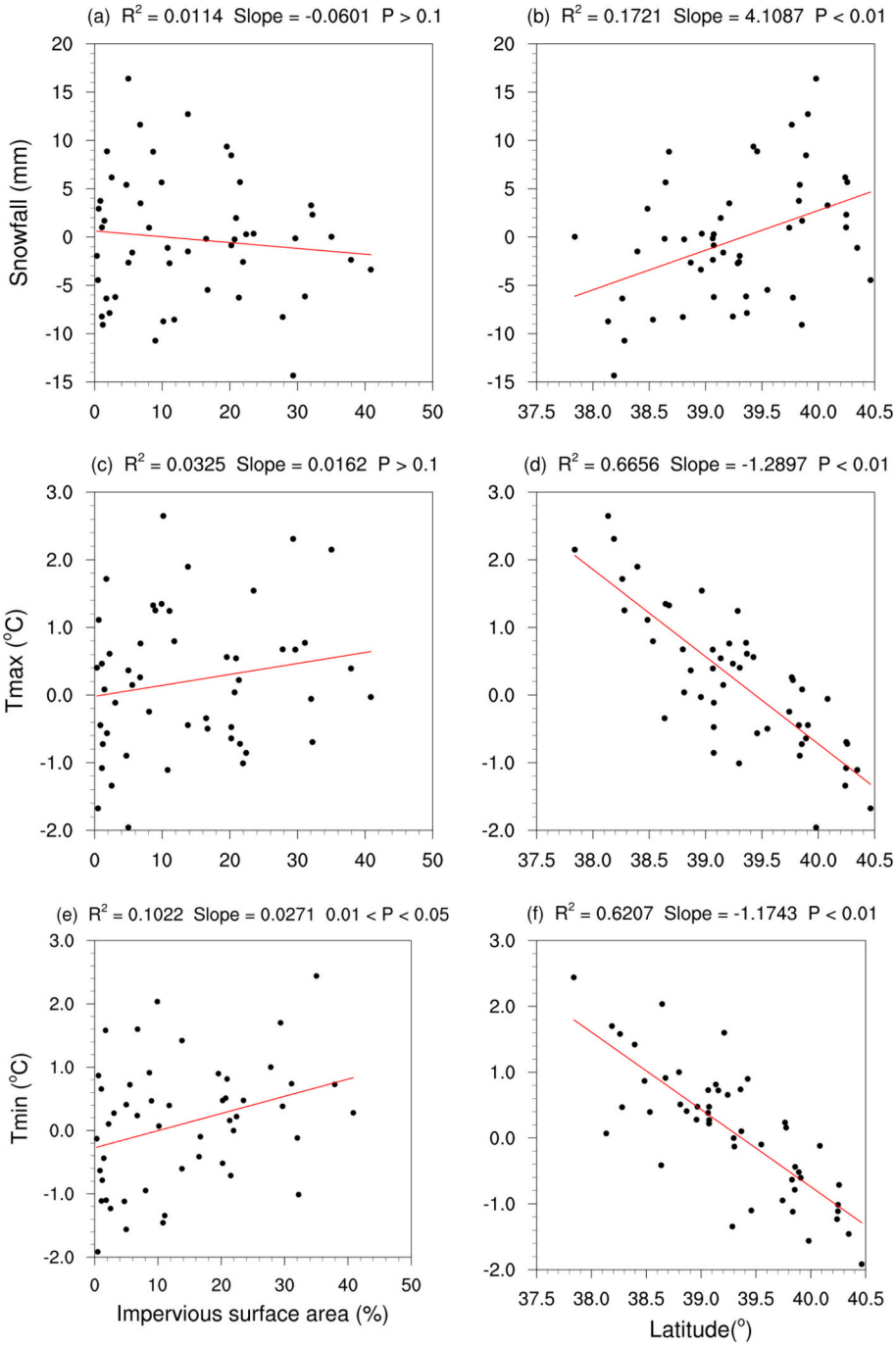


**Fig. 5.** The unary linear regression results between independent variables (Imp and Lat) and dependent variables (Snowfall, Tmax and Tmin) in Kansas City.

In the following, We use Kansas City, Boston, and Denver as examples to demonstrate the relations between dependent variables (precipitation and temperatures) and independent variables (e.g., *Imp* and *Lat*), which can help us interpret the results shown in Table 3. Fig. 5 shows the unary linear regression between independent variables (*Imp* and *Lat*) and dependent variables (*Snowfall*, $T_{max}$ and $T_{min}$) in Kansas City. Since it is an inland city, only two independent variables (*Imp* and *Lat*) are analyzed. There is a significantly positive correlation between the impervious surface fraction and $T_{min}$ (Fig. 5e). Although the correlation between the impervious surface fraction and another two dependent variables (*Snowfall* and $T_{max}$) is weak ($P > 0.1$), we can still see that increases in impervious surface fraction lead to increases in $T_{max}$ increase and reductions in *Snowfall* (Fig. 5a and c). Both snowfall and temperature show significant correlations with latitude ($P < 0.01$). As latitude increase, snowfall shows significant increases, while temperature is significantly reduce (Fig. 5b, d and f).

Another independent variable *Dis* (Distance from the coast) is added for the regression analysis in the coastal city Boston (Fig. 6b, e and h). There is a significantly positive correlation between the impervious surface fraction and temperature (Fig. 6d and g). Compared to temperature, the correlation between the impervious surface fraction and snowfall is weaker ($P > 0.1$). However, we can still see

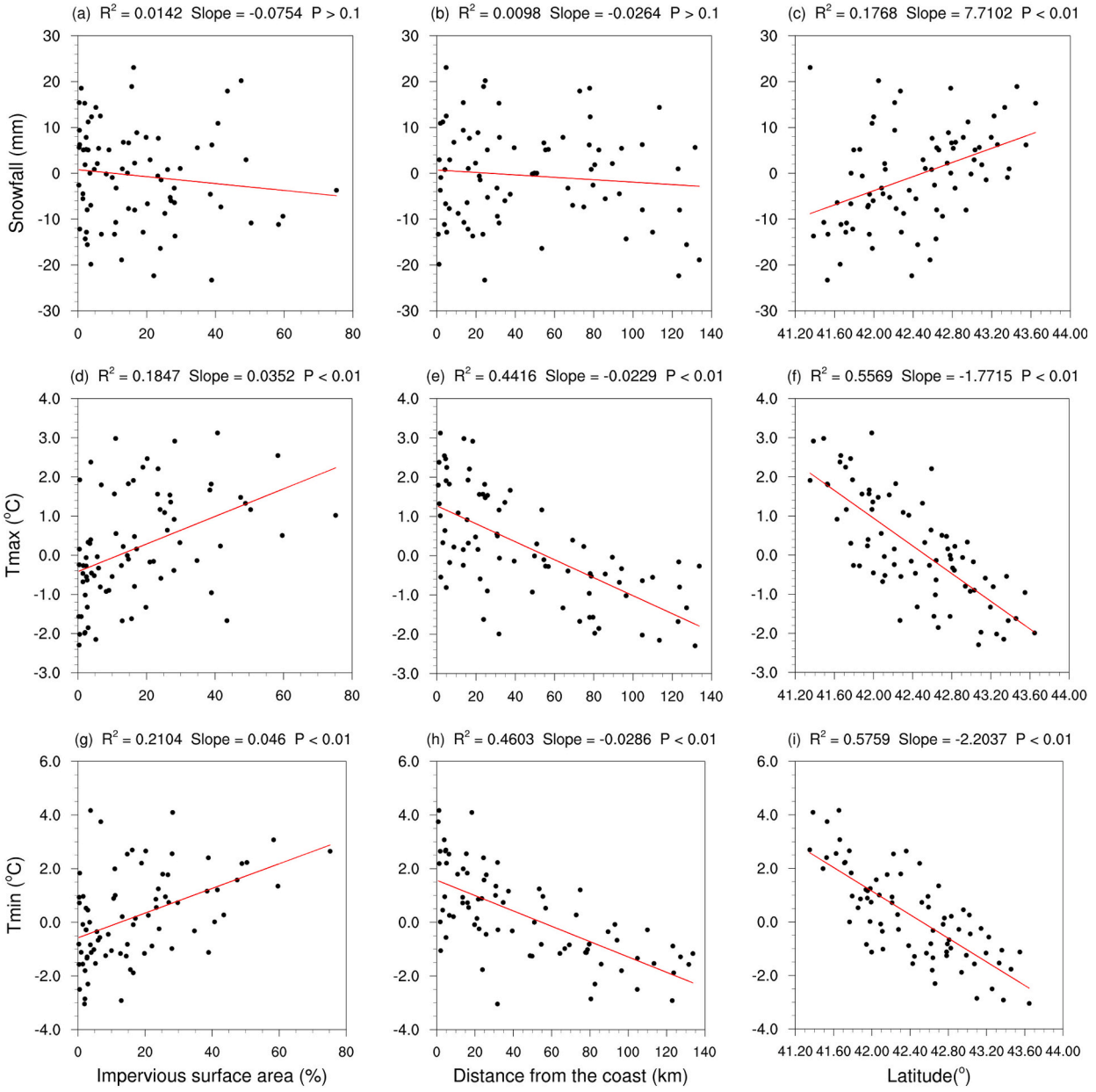


**Fig. 6.** The unary linear regression results between independent variables (Imp, Dis and Lat) and dependent variables (Snowfall, Tmax and Tmin) in Boston.

that increases in impervious surface fraction lead to snowfall reduction (Fig. 6a). Generally speaking, there should be a negative correlation between snowfall and temperature as shown in Table 2. In other words, the correlation between the two dependent variables (snowfall and temperature) and the same independent variable should be opposite. However, the correlation between the two dependent variables (snowfall and temperature) and the distance from the coastline shows the same sign (all are negatively correlated, see Fig. 6b, e and h). These correlations indicate that the further away from the coastline, the lower the temperature, and the less the snowfall. This is because snowfall is affected not only by temperature, but also by water vapor likely provided by the Atlantic Ocean. It is precisely because of the complexity of the factors affecting snowfall in coastal cities that the correlation between snowfall and a single independent variable (e.g., *Imp* and *Dis*) is not significant against the null hypothesis (Fig. 6a and b). We note that latitude is still a key factor affecting snowfall and temperature for Boston (Fig. 6c, f and i).

In Denver, the negative correlation between snowfall and impervious surface fraction is more significant (Fig. 7a, $0.01 < P < 0.05$). Moreover, as Denver's climate is greatly affected by the mountainous terrain, the correlation between the three dependent variables (*Snowfall*, $T_{max}$ and $T_{min}$) and latitude is not significant (Fig. 7b, e and h). The altitude of each station over Denver varies greatly. Therefore, we add another independent variable *Alt* (Altitude, in meters above sea level) in our analysis (Fig. 7c, f and i). The other

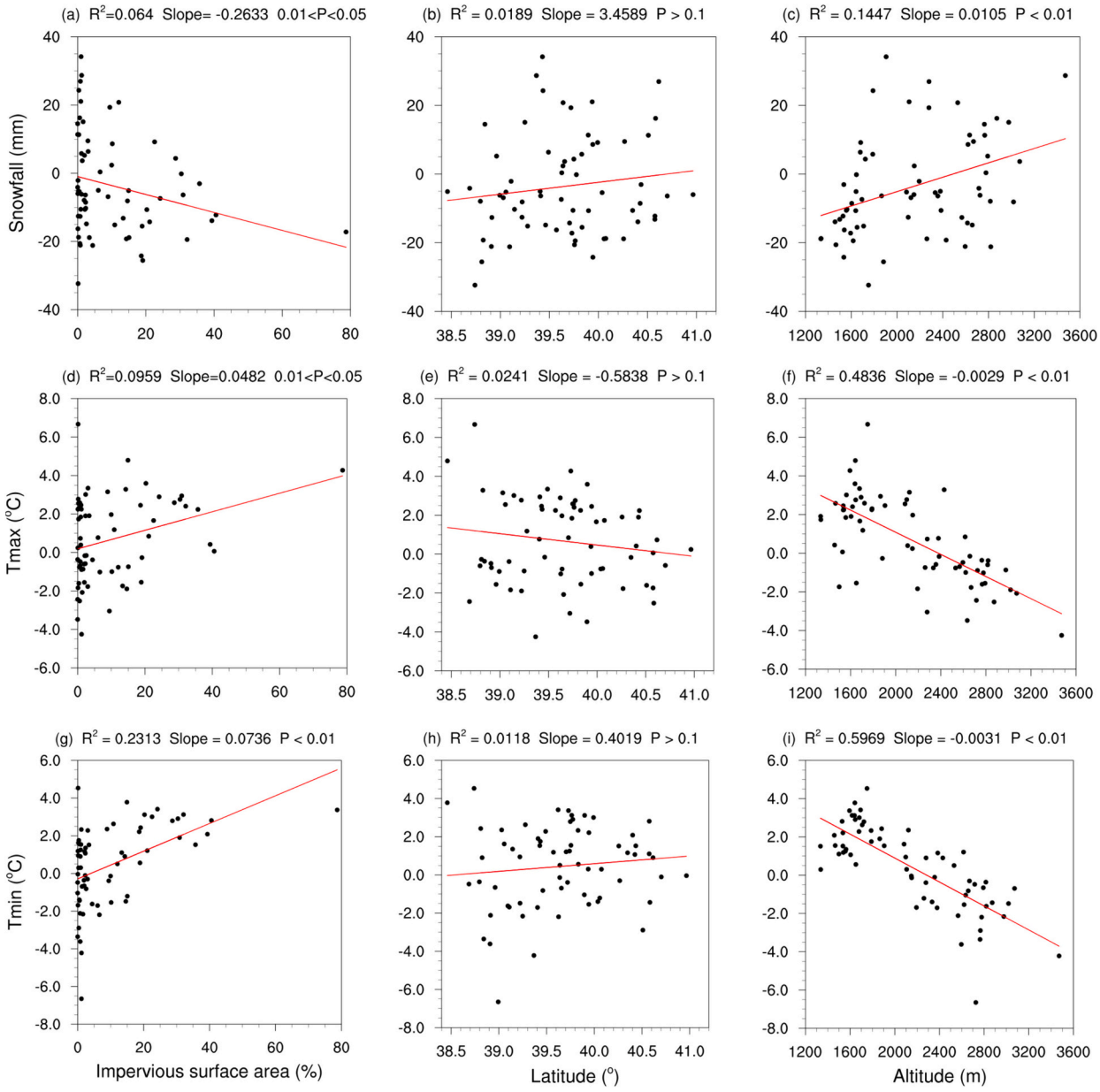


**Fig. 7.** The unary linear regression results between independent variables (Imp, Lat and Altitude) and dependent variables (Snowfall, Tmax and Tmin) in Denver.

cities do not show large variations in the altitude for the analyzed stations and hence the same analysis is not repeated for the other cities. The results suggest that the correlation between the three dependent variables (*Snowfall*, $T_{max}$ and $T_{min}$) and altitude is significant ($P < 0.01$). As altitude increases, snowfall shows significant increases, while temperatures are significantly reduced.

In summary, snowfall was negatively correlated with temperatures while rainfall was positively correlated with temperatures. For most cities, the impervious surface fraction was positively correlated with temperatures and negatively correlated with snowfall, indicating that the impervious surface fraction was an important factor affecting both temperatures and snowfall, especially for inland cities. For coastal cities, the distance from the coastline was a more important factor affecting snowfall than the impervious surface

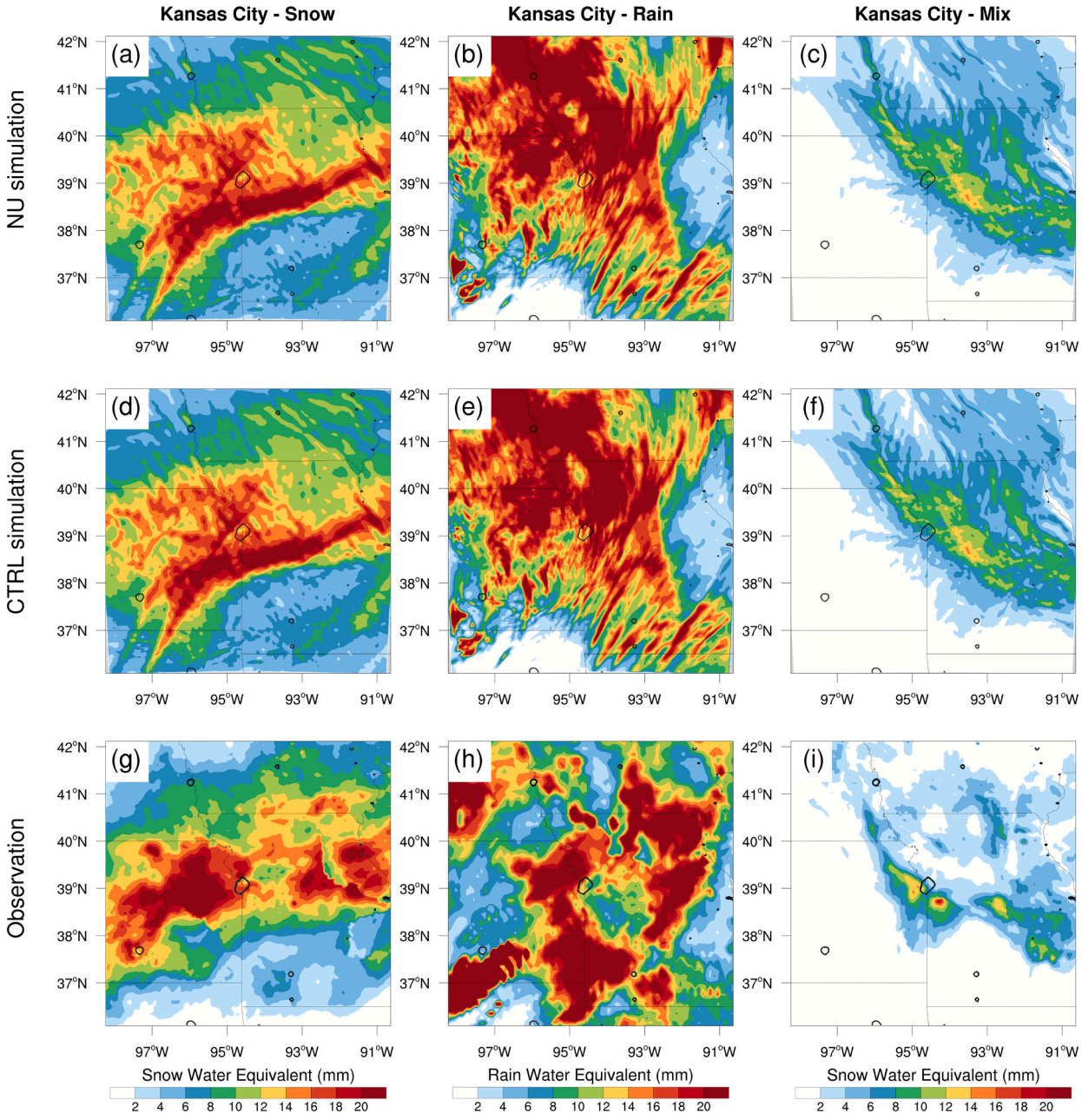


**Fig. 8.** The simulated 24-h accumulation snowfall (snow water equivalent, mm) of the No-Urban (NU) simulation (top row), CTRL simulation (middle row) and observation (bottom row) for (a, d, g) Kansas City - Snow and (b, e, h) Kansas City - Mix. The 24-h period is from 2014 to 02-04 06 LT to 2014-02-05 06 LT for Kansas City - Snow and from 2010 to 02-05 06 LT to 2010-02-06 06 LT for Kansas City - Mix. And the simulated 48-h accumulation rainfall (mm) of the No-Urban (NU) simulation (top row), CTRL simulation (middle row) and observation (bottom row) for (b, g, l) Kansas City. The 48-h period is from 2010 to 03-08 18 LT to 2010-03-10 18 LT for Kansas City - Rain. The NU and CTRL simulation show results from Domain 2.

fraction. However, the distance to coast could be either positively or negatively correlated with snowfall. Latitude was a key factor affecting temperatures. But the correlation between snowfall and latitude was not significant across the cities examined here.

One caveat of these statistical analyses is that with multiple variables affecting snowfall, the correlation between snowfall and independent variables was often weak. In particular, the relation between snowfall and impervious surface fraction was weak. Thus we carried out numerical simulations to elucidate how urban land affects winter precipitation.

### 3.2. Numerical simulations

As mentioned in Section 2, we also investigated the impacts of urban land on winter precipitation using numerical simulations (three case studies over Kansas City). Three cases (i.e. Kansas City - Snow, Kansas City - Rain and Kansas City - Mix) over Kansas City were simulated to show urban impacts on different types of winter precipitation. Before discussing the results from numerical simulations, it is important to acknowledge that the sample size was limited. Hence, our findings should be interpreted cautiously. However, the consistency between the numerical simulation results and the statistical results, which will be highlighted below, gave us confidence in our findings.

#### 3.2.1. Model performance

The simulated 24-h accumulation snowfall (represented by snow water equivalent, for snow only and mixed precipitation events) or simulated 48-h accumulation rainfall (for rain only event) in both No-Urban (NU) and CTRL scenarios were spatially consistent with the observations for all three events (Fig. 8, Table 4), although light and moderate precipitation was overestimated. The distribution of the snow band or rain was well captured by the model, with the caveat that there seemed to be a slight westward shift for the Kansas City - Rain case (Fig. 4g and i) and a slight northward shift for the Kansas City - Mix case (Fig. 8h and m). The snowfall and rainfall intensity was also comparable between the CTRL simulation and observation (Table 4). These results suggested that the model reasonably captured the precipitation over these three cases. Thus, comparisons between the CTRL and NU scenarios could shed light on the impacts of urban land on the spatial and temporal pattern of winter precipitation.

#### 3.2.2. Spatial variability

Fig. 9 showed the synoptic conditions (i.e., temperature, geopotential height, and wind field at 850 hPa) at four times during the 24-h precipitation period for the three events. For Kansas City - Snow, a low-pressure system moved from southwest to northeast during this period, with cooling effects and stronger winds from east to west over the city (Fig. 9a, Fig. 9d, Fig. 9g and Fig. 9j). For Kansas City - Rain, the center of a low-pressure system to the west of the city moved across the city area, with stronger winds from south to north (Fig. 9b, Fig. 9e, Fig. 9h and Fig. 9k). For Kansas City - Mix, a stationary surface cyclone was strengthened to the east of Kansas City, with cooling effects and stronger winds from north to south (Fig. 9c, Fig. 9f, Fig. 9i and Fig. 9l).

Fig. 10 showed the differences between the CTRL and NU scenarios (CTRL minus NU, representing the impacts of urban land) in terms of the 2-m air temperature, 2-m specific humidity and 10-m wind speed averaged over the entire simulation period. For different types of precipitation over Kansas city, similar warming effects were seen in all three cases (Fig. 10a, Fig. 10b, Fig. 10c). However, the three cases showed different changes of the 2-m specific humidity. The urban land had small effects on the 2-m specific humidity within the city area, but caused a slight increase in specific humidity (0.1 g/kg) in the downwind area of the city in the snow only case and the mixed precipitation case (Fig. 10d and Fig. 10f). While in the rainfall only case, the urban land reduced the specific humidity (0.15 g/kg) within the city area (Fig. 10e). In addition to the thermodynamic perturbations induced by urban land, noticeable perturbations existed in the near-surface wind field due to increases in surface roughness as well as buoyancy fluxes. There was a decrease in near-surface wind speed in all three cases in Kansas City, consistent with the increases in surface roughness and buoyancy fluxes (Fig. 10g, Fig. 10h, Fig. 10i). It was noteworthy that the decrease of near-surface wind speed occurred over the downwind area of Kansas City in the snow only case and the mixed precipitation case (Fig. 10g and Fig. 10i).

Fig. 11 showed the differences of the accumulated snowfall, rainfall and total precipitation between CTRL and NU scenarios for the three cases. Also shown were the wind fields from CTRL. For all cases in Kansas City, there was no abrupt change in the magnitude and direction of wind over the city area (Fig. 11a, Fig. 11b, Fig. 11c).

For the snowfall only case in Kansas City, snowfall decreased by about 1 mm over the downwind area and increased by about 1 mm over the upwind area of the city (Fig. 11a). Changes in wind speed and temperature caused by urbanization may be the cause of this

**Table 4**
The 24-h area-average and maximum snowfall accumulations (snow water equivalent, mm) for Kansas City - Snow, Kansas City - Mix and the 48-h area-average and maximum rainfall accumulations (mm) for Kansas City - Rain in both domain 2 and domain 3. The 24-h period and 48-h period are the same as Fig. 4.

| | Domain 2 | | | | Domain 3 | | | |
|---|---|---|---|---|---|---|---|---|
| | Area-average (mm) | | Maximum (mm) | | Area-average (mm) | | Maximum (mm) | |
| | Simulation | Observation | Simulation | Observation | Simulation | Observation | Simulation | Observation |
| Kansas City - Snow | 10.05 | 9.11 | 27.14 | 30.67 | 16.70 | 14.97 | 27.27 | 30.56 |
| Kansas City - Rain | 13.11 | 12.95 | 45.40 | 54.25 | 18.34 | 15.61 | 40.94 | 33.73 |
| Kansas City - Mix | 3.55 | 1.92 | 14.93 | 20.88 | 6.64 | 4.73 | 14.77 | 21.03 |

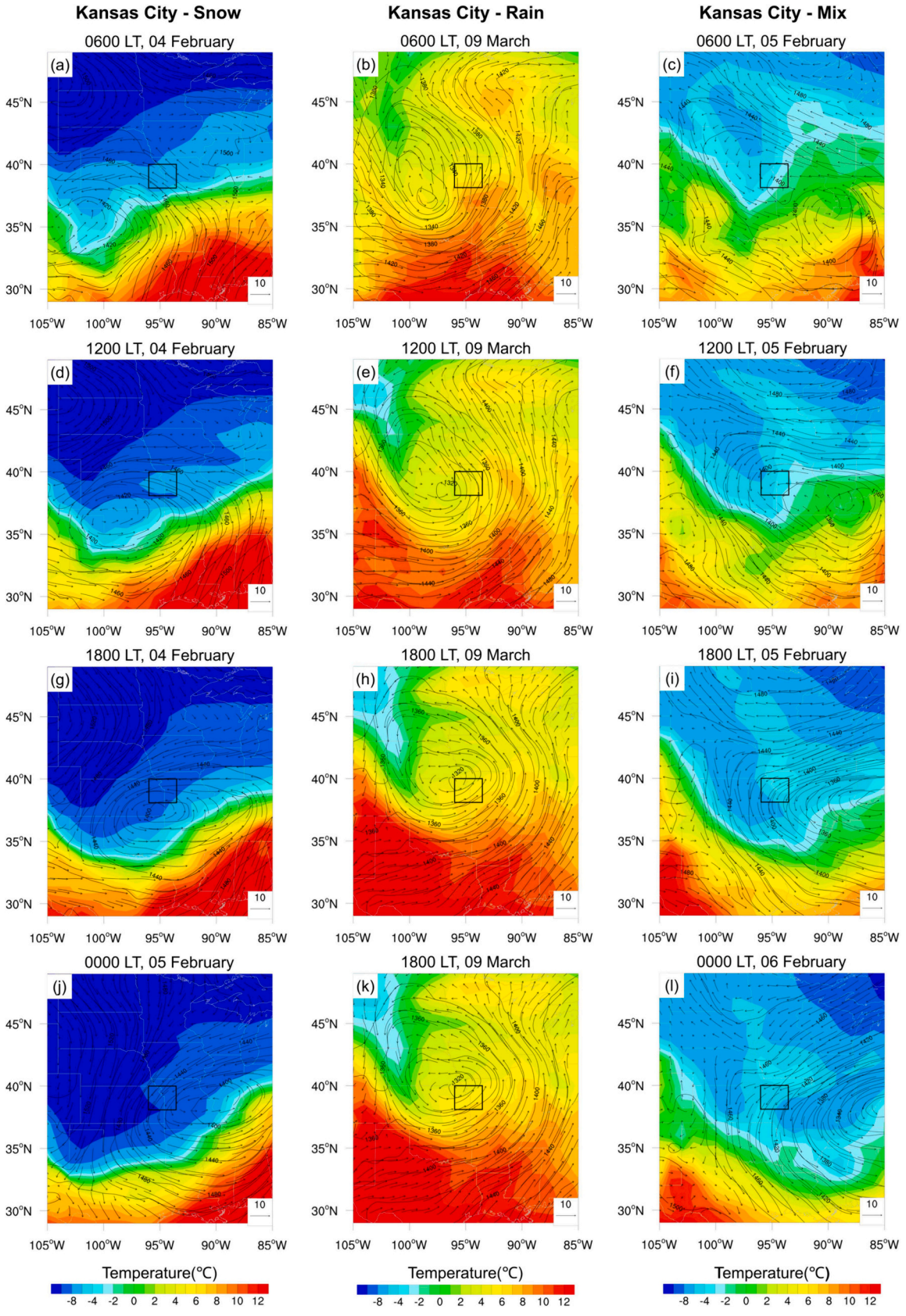


*(caption on next page)*

**Fig. 9.** The synoptic conditions at 850 hpa during the 24-h precipitation period for (a, d, g, j) Kansas City - Snow, (b, e, h, k) Kansas City - Rain and (c, f, i, l) Kansas City - Mix. The 24-h precipitation period was from 2014 to 02-04 06 LT to 2014-02-05 06 LT for Kansas City - Snow, 2010-03-09 06 LT to 2010-03-10 06 LT for Kansas City - Rain and 2010-02-05 06 LT to 2010-02-06 06 LT for Kansas City - Mix. The shaded colour indicates air temperature (°C), the contours denote geopotential height (m), and the arrows denote wind fields (m/s). The data are taken from the National Center for Environmental Prediction (NCEP) Global Final Analysis (FNL) fields. The black squares indicate the domain 3 in three cases.

phenomenon. In the upwind area of the city, decrease in near-surface wind speed dominated and led to snowfall accumulation, while in the downwind area of the city, the warming effect (Fig. 10a) dominated and caused the negative snowfall anomaly. The impact distance on snowfall was relatively large (about 100 km) outside the city.

Unlike the clear anomaly in the snow only case, the rainfall changes were complicated in the rainfall only case. As the center of the low-pressure system moved over Kansas City during the simulation period, a convergence zone occurred to the north of the city (Fig. 11e) and the regional circulation in the center was significantly affected by urban land (Fig. 10h). As a result, the urban land

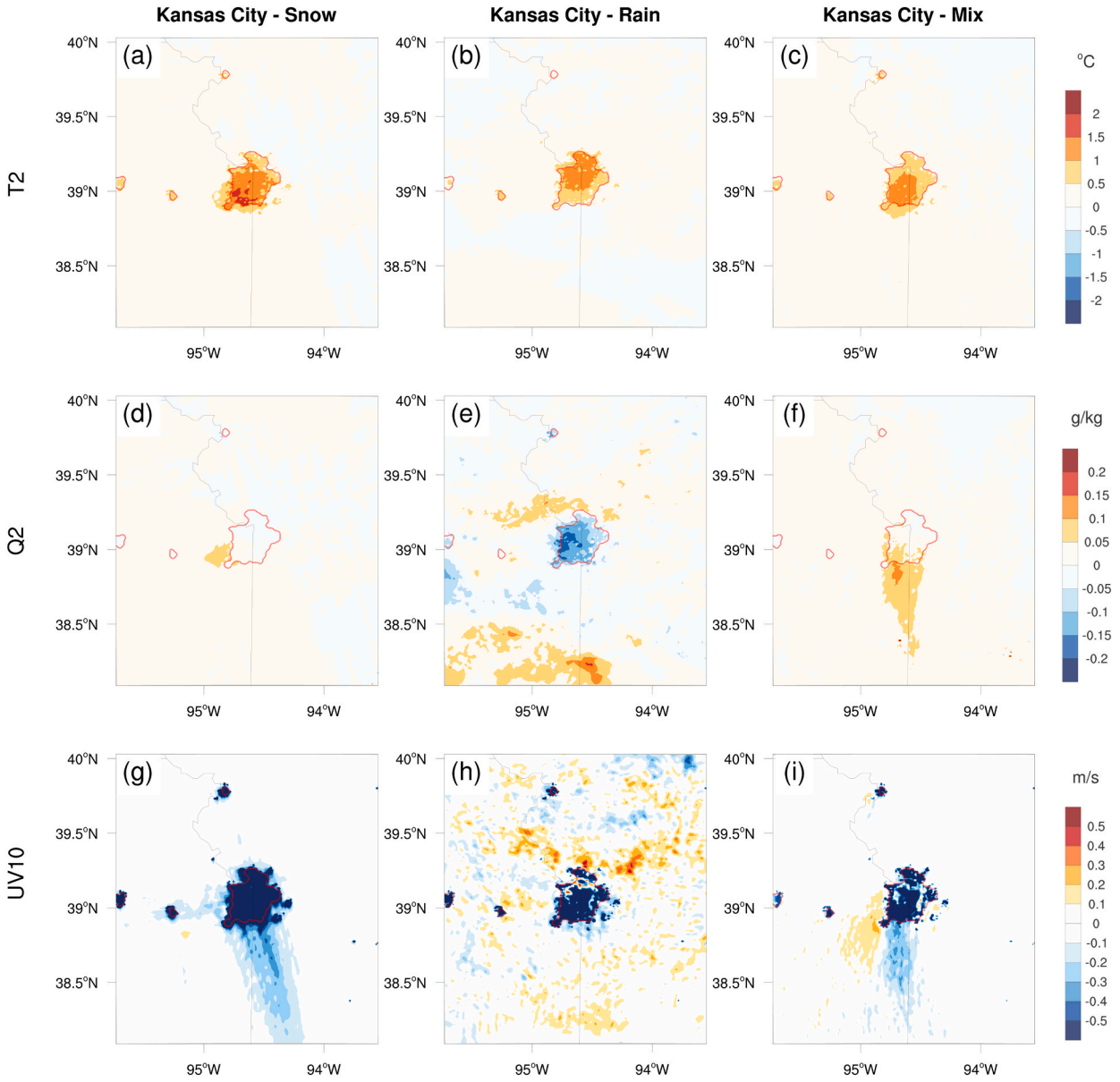


**Fig. 10.** Differences of 2-m temperature (top row, °C), 2-m specific humidity (middle row, g/kg) and 10-m wind speed (bottom row, m/s) between CTRL and NU scenarios averaged over the simulation period for Kansas City - Snow, Kansas City - Rain and Kansas City - Mix from left column to right column. The red polygon represents the urban boundary. (For interpretation of the references to colour in this figure legend, the reader is referred to the web version of this article.)

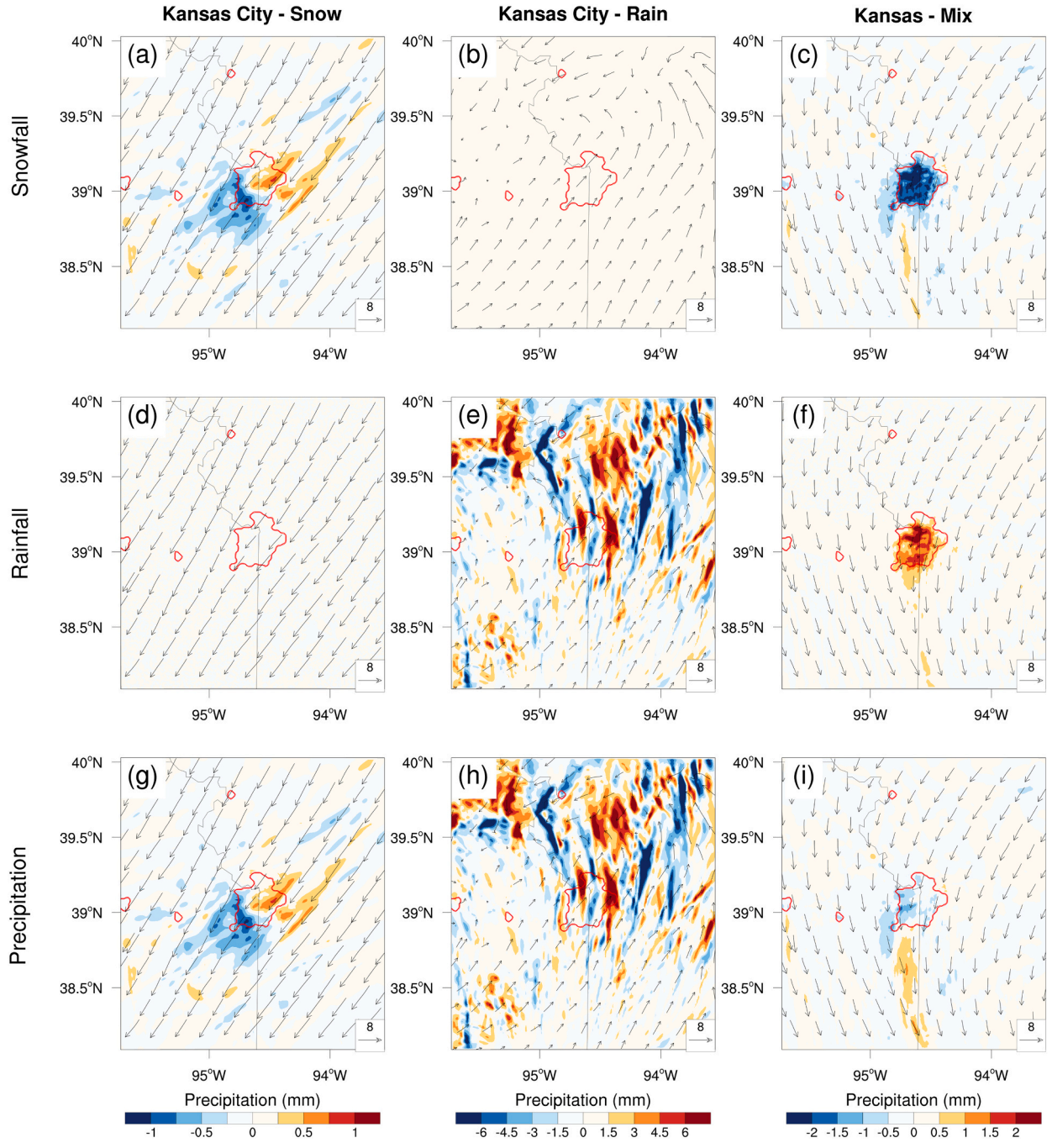


**Fig. 11.** Differences of accumulated snowfall (top row), rainfall (middle row) and precipitation (bottom row) between CTRL and NU scenarios over the simulation period for (a, d, g) Kansas City - Snow, (b, e, h) Kansas City - Rain and (c, f, i) Kansas City - Mix. Vectors represent 10-m wind fields at 2014-02-04 18 LT (Kansas City - Snow), 2010-03-09 18 LT (Kansas City - Rain) and 2010-02-05 18 LT (Kansas City - Mix). The red polygon represents the urban boundary. (For interpretation of the references to colour in this figure legend, the reader is referred to the web version of this article.)

influenced the rainfall in the downwind region of the urban boundary with a magnitude of about 6 mm, while a slight decrease (about 3 mm) occurred over some part of the city. In addition, rainfall over the convergence area showed complex anomalies.

Both rainfall and snowfall in Kansas City - Mix were altered by the urban land, with snowfall decreased by about 2 mm (Fig. 11c) and rainfall increased by about 2 mm (Fig. 11f). In addition, the urban land influenced the snowfall and rainfall in the downwind region for Kansas City with a magnitude of about 1 mm. The impact distance on rainfall was relatively large (about 100 km), while the

impact distance on snowfall was relatively small (about 30 km). In terms of the total precipitation, urban land showed a small impact, with some decreases in the immediate downwind region and some increases in the distant downwind region (Fig. 11i). The changes in rainfall and snowfall were spatially different (Fig. 11c and Fig. 11f). This highlights the importance of separating precipitation into rainfall and snowfall in order to clearly identify urban impacts on winter precipitation. Overall, since Kansas City is a typical inland city with no complex terrain or land-water boundary, the impact of urbanization on winter precipitation was not compounded by other geographical factors.

### 3.2.3. *Temporal variability*

For the three events, time series of hourly snowfall rates, rainfall rates and total precipitation (the sum of snowfall and rainfall) rates averaged over urban grid cells were shown in Fig. 12.

For Kansas City - Snow, the total snowfall value during the entire simulation period was 19.2 mm. As for Kansas City - Rain, the total rainfall was 17.1 mm. The total precipitation in the mixed precipitation event was dominated by snowfall, with mixed precipitation during some periods. For Kansas City - Mix, the total precipitation value during the entire simulation period was 11 mm, of which snowfall accounted for 93%. In terms of hourly precipitation rate, Kansas City - Rain had the largest value, reaching 2.4 mm/h, while Kansas City - Mix showed the lowest hourly precipitation rate, with the maximum hourly precipitation rate less than 1.0 mm/h.

The snow only event in Kansas City lasted for 30 h (Fig. 12a). The snowfall was reduced during the first 20 h and increased during the last 10 h (Fig. 12d). There were two episodes of rainfall in Kansas City - Rain (Fig. 12b). For the first episode, the impacts of urban land (again represented by the differences between the CTRL and NU scenarios) were quite weak, while a large increase of rainfall was shown in the second episode, which was selected for further analysis (Fig. 12e).

The mixed precipitation event in Kansas City lasted about 40 h, with 15-h mixed precipitation (Fig. 12c). During the period of mixed precipitation, the impacts of urban land were quite strong (Fig. 12f). Overall, the rainfall was increased and the snowfall was reduced. The magnitude of snowfall reduction was greater than that of rainfall increase, resulting in a slight decrease in the total precipitation. During the periods when there was only snowfall, the differences between the two scenarios were small.

Fig. 13 further showed the differences between CTRL and NU scenarios in terms of vertical distributions of temperature and moisture variables, which have been averaged over all urban grids, during the key precipitation periods (shaded regions in Fig. 12). The vertical extent of temperature increase was approximately 500 m from the surface, corresponding to the typical atmospheric boundary layer height. The temperature increase was observed for all 3 events. For Kansas City - Snow, the temperature increased by about 0.1 $^{\circ}C$ below 500 m and decreased by about 0.1 $^{\circ}C$ between 500 m to 1 km. For Kansas City - Rain and Kansas City - Mix, the temperature increases by about 0.1 $^{\circ}C$ below 500 m. As a result, all hydrometeors were affected, with the strongest impact on ice and snow.

For the snow only event in Kansas City (Fig. 13 a, d, g, j, m), it was noteworthy that the warming effect of urban land only occurred during the first 20 h, in which ice and snow were reduced near the surface. However, they were increased slightly above 200 m. This was likely because the increase in temperature helped melt ice and snow at the surface, while at the same time the updraft of warm

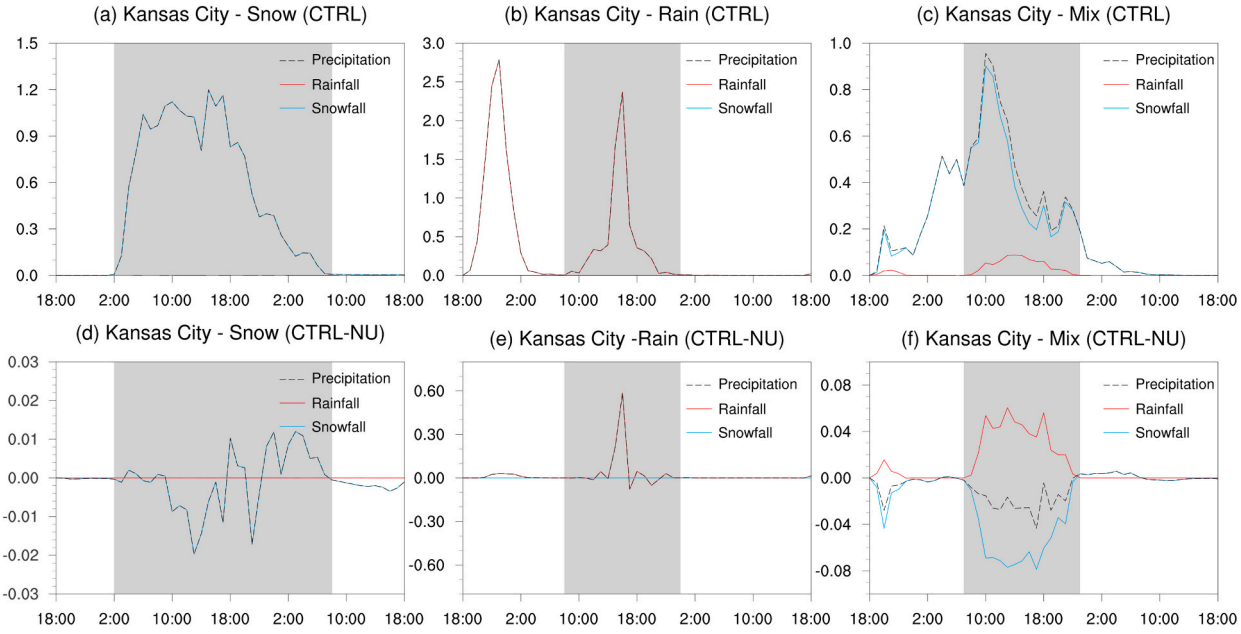


**Fig. 12.** Time series of hourly precipitation rates (mm/h) averaged over urban grid cells (see Fig. 3) for (a, d) Kansas City - Snow, (b, e) Kansas City - Rain and (c, f) Kansas City - Mix. (a-c) are the CTRL simulation results. (d-f) are the differences between CTRL and NU scenarios. The gray shading area represents the precipitation phase for further analysis.

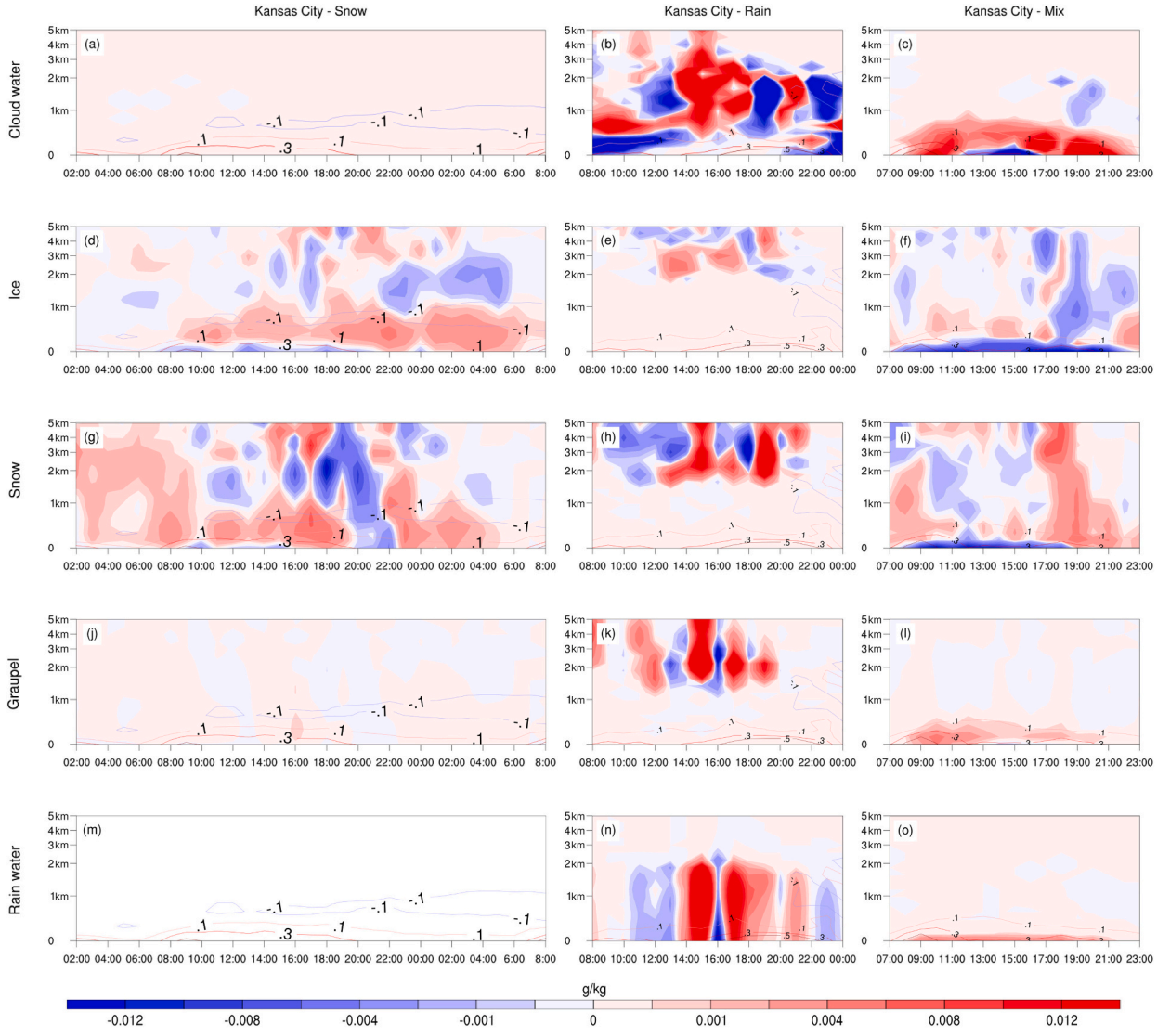


**Fig. 13.** Vertical distribution of differences between CTRL and NU scenarios in terms of moisture variables (cloud water, ice, snow, graupel and rain water; shade; g/kg) and temperature (contour at every 0.2 K) during the gray shading precipitation period in Fig. 12 for Kansas City - Snow, Kansas City - Rain and Kansas City - Mix. The results are averaged over urban grid cells.

moist air parcel condensed at higher altitudes, facilitating the formation of ice and snow. The urban warming effect disappeared in the late snowfall period and led to increase of ice and snowfall.

As for the rain only event in Kansas City - Rain (Fig. 13 b, e, h, k, n), the anomalies of rain were consistent with the warming effect. When the warming effect was enhanced (from 1400 LT to 2200 LT), rain was increased significantly; while during other period, rain was reduced slightly.

For the mixed precipitation event in Kansas City (Fig. 13 c, f, i, l, o), when the precipitation peak was observed (around 1000 LT on the first day), in the altitude range where the temperature was enhanced (below 500 m or so), the ice and snow decreased while the graupel and rain water increased. During the mixed precipitation period, the warming effect of urban land was strong and the changes of ice, snow and rain were consistent with the snow only event and the rain only event results, respectively.

Putting together results of temporal variability from three different types of winter precipitation in Kansas City, we could conclude that changes of snowfall and rainfall were significantly related to the temperature changes. When the atmosphere was heated up by urban land, snowfall was reduced while rainfall and graupel were increased. These findings were broadly consistent with our statistical analyses. For snow only events, the warming effect occurred during the early stage and disappeared with the accumulation of snow, thus snowfall decreased in the early stage and increased in the later stage, at least for Kansas City - Snow. As for rain only events, the warming effect occurred during the later stage, resulting in the increase of rainfall (e.g., in Kansas City - Rain). For mix precipitation

case, the warming effect led to the changes of ice, snow and rain, which were consistent with the snow only event and the rain only event.

#### 3.2.4. Results from the season-long simulation

Fig. 14 showed the differences between the CTRL and NU scenarios (CTRL minus NU, representing the impacts of urban land) in terms of the accumulated snowfall, rainfall and total precipitation during the entire period of the season-long simulation. In the CTRL case, the total snowfall was 151.33 mm, while the total rainfall was 143.28 mm. The accumulated snowfall was reduced by urban land over the inner city area (up to 15 mm) and the eastern and southern surrounding areas, while an increased snowfall band (up to 12 mm) was observed to the northwest of the city (Fig. 14 a). As for the areas farther away from the city, reductions of snowfall occurred to the southwest of the city, and slight increases occurred to the south of the city. For most part of the domain, rainfall was increased by urban land, especially over the areas where snowfall was reduced (Fig. 14 b). For the total precipitation (Fig. 14 c), the changes showed complex distributions. A band of total precipitation increase was located to the northwest of the city, coinciding with the band of snow increase; while reductions of precipitation occurred near the city and over the east and southwest of the city. In the southeast region farther away from the city, precipitation was increased significantly.

Overall, the existence of urban land leads to reductions of accumulated snowfall and increases of accumulated rainfall over the city area. As for the total precipitation within the city, the anomalies were opposite in different regions - increase in the western part and decrease in the eastern part. Meanwhile, the existence of urban also has impacts on the precipitation outside the city. The snowfall anomalies were different at different locations outside the city but with good consistency, while rainfall was increased over most areas in the domain.

## 4. Conclusion

In this study, we carried out statistical analyses to quantify the influence of impervious surface fraction on winter precipitation across 12 major U.S. cities. Three types of winter precipitation (snow only, rain only and mixed precipitation) over Kansas City were selected in modeling simulation to elucidate the physical processes through which urban land influences winter precipitation. The main findings were summarized below.

(1) Snowfall was significantly negatively correlated with air temperatures in the studied cities. Meanwhile, rainfall was significantly positively correlated with air temperatures. Snowfall and impervious surface fraction were generally negatively correlated. The correlation between snowfall and impervious surface fraction was more significant for inland cities than for coastal and lakeside cities. For coastal cities, snowfall was significantly affected by the distance to coastline. Latitude was found to affect daily maximum temperature more than daily minimum temperature, while the impervious surface fraction significantly affected daily minimum temperature. The correlation between latitude and snowfall was nonetheless not significant. In areas with strong altitude variations, temperature was also strongly correlated with altitudes.
(2) Based on simulation results of three precipitation events, when urban land was replaced by the dominant rural land cover type in the surrounding, near-surface air temperature, humidity, wind speed, and various hydrometers in the atmospheric column were affected. In the near-surface atmosphere (within 500 m high), the warming effect of urban land caused reductions in ice and snow and increases in graupel and rain water. For snow only precipitation, the warming effect was stronger in early stage, leading to reduction of snowfall. For rain only precipitation, the warming effect was stronger in late stage, leading to increase of rainfall. In mixed precipitation events, the warming effect occurred resulted in reductions in snowfall and increases in rainfall and graupel. When the warming effect weakened, the reductions of wind speed caused by increases in surface roughness and buoyancy fluxes could lead to the increase of both snowfall and rainfall. The season-long simulation over Kansas City further testified the role of urban land, which led to less snowfall and more rainfall in inner city over the winter season in 2009–2010. For the surrounding area of the city, the impact of urban was visible but complex.
(3) Combining the results of statistical analyses and numerical simulations, we conclude that the impervious surface fraction or the urban land as in the case of numerical simulations plays an important role in affecting winter precipitation. The urban influence becomes more pronounced during mixed-precipitation events, where the urban-induced temperature rise results in reduced snowfall and increased rainfall. Specifically, statistical analyses suggested that higher impervious surface fraction was generally associated with higher air temperatures, less snowfall, and more rainfall. Simulations results suggested that the higher temperatures caused by urban land were not only found at the surface, but also in the atmospheric boundary layer (especially below 500 m), leading to changes in hydrometers. The changes in hydrometers were consistent with decreases of snowfall and increases of rainfall as in the statistical analyses.

Based on statistical analyses of multi-year observation data and both case and long-term studies with WRF simulations, this study provides evidence on the influence of impervious surface fraction (urban land) on winter precipitation. However, as we have noted earlier, only three winter precipitation events were simulated for one city, and thus the generalization of our numerical results needs to be practiced with caution. Future modeling studies on events with diverse synoptic conditions are needed. For cities with mountainous terrain or next to water bodies, further modeling studies on how their effects interact with the urban effects may shed new insights. In consideration of the complexity associated with winter precipitation, studies on the fundamental physical processes such as land surface/ boundary layer/ microphysical processes involved in winter precipitation events are needed. With existence of ice, snow, graupel and other moisture variables, the complex microphysical processes of snowfall were quite challenging in the simulation and

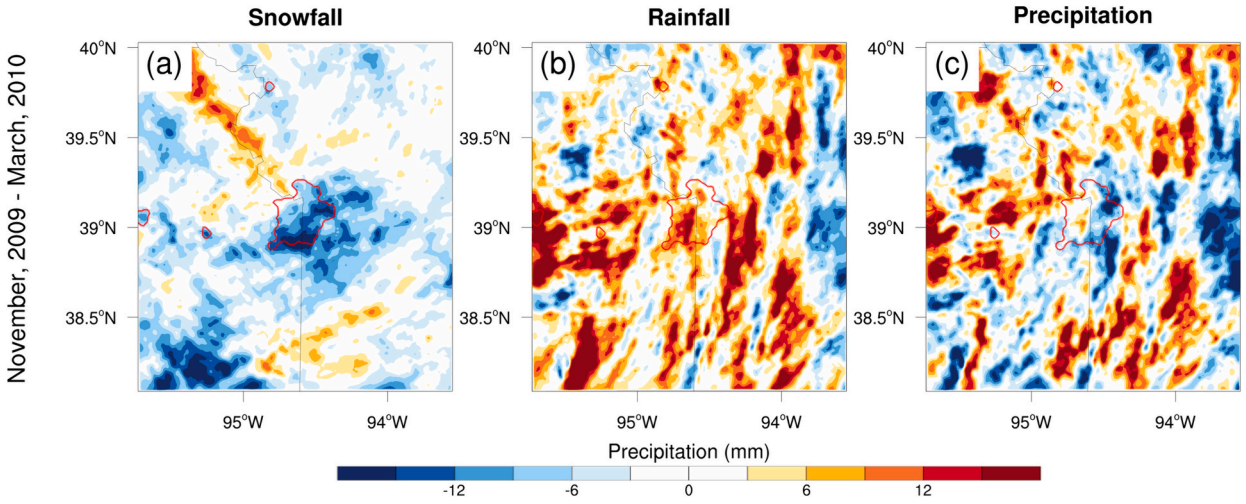


**Fig. 14.** Differences of accumulated snowfall (a), rainfall (b) and precipitation (c) between CTRL and NU scenarios of the winter-season simulation over Kansas City. The red polygon represents the urban boundary. (For interpretation of the references to colour in this figure legend, the reader is referred to the web version of this article.)

research. In addition to the spatial and temporal distribution changes of these variables caused by city in this study, the transformation relationship of various moisture variables and the influencing factors in the snowfall process can be further studied. Last but not least, more studies using observations to statistically quantify the urban effects in other regions and using observations to evaluate numerical simulations are strongly encouraged.

## Data statement

The datasets analyzed in the study and the model settings are included in the article. Further inquiries can be directed to the corresponding author.

## Declaration of competing interest

The authors declare that they have no known competing financial interests or personal relationships that could have appeared to influence the work reported in this paper.

## Data availability

Data will be made available on request.

## Acknowledgments

The study is supported by The Ministry of Science and Technology of the People's Republic of China (2022YFC3090604) and the Open Research Fund Program of State Key Laboratory of Hydroscience and Engineering (sklhse-2020-A-02). Y.L. also acknowledges support from the Natural Science Foundation of China (52009055).

## References

Bokwa, A., 2009. Effects of air pollution on precipitation in Kraków (Cracow), Poland in the years 1971–2005. Theor. Appl. Climatol. 101, 289–302. https://doi.org/10.1007/s00704-009-0209-7.

Bornstein, R., LeRoy, M., 1990. Urban barrier effects on convective and frontal thunderstorms. In: Extended Abstracts, Fourth Conf. on Mesoscale Processes, pp. 120–121.

Bornstein, R., Lin, Q., 2000. Urban heat islands and summertime convective thunderstorms in Atlanta: three case studies. Atmos. Environ. 34, 507–516. https://doi.org/10.1016/s1352-2310(99)00374-x.

Changnon, S.A., 2004. Urban effects on winter snowfall at Chicago and St. Louis. Bull. Illinois Geogr. Soc. 46, 3–12.

Changnon Jr., S.A., 1975. The paradox of planned weather modification. Bull. Am. Meteorol. Soc. 56, 27–37.

Changnon Jr., S.A., Huff, F.A., Semonin, R.G., 1971. METROMEX: an investigation of inadvertent weather modification. Bull. Am. Meteorol. Soc. 52, 958–968.

Chen, F., Dudhia, J., 2001. Coupling an advanced land surface–hydrology model with the Penn State–NCAR MM5 modeling system. Part I: model implementation and sensitivity. Mon. Weather Rev. 129, 569–585. https://doi.org/10.1175/1520-0493(2001)129¡0569:caalsh¿2.0.co;2.

Chen, F., Kusaka, H., Bornstein, R., Ching, J., Grimmond, C.S.B., Grossman-Clarke, S., Loridan, T., Manning, K.W., Martilli, A., Miao, S., Sailor, D., Salamanca, F.P., Taha, H., Tewari, M., Wang, X., Wyszogrodzki, A.A., Zhang, C., 2011. The integrated WRF/urban modelling system: development, evaluation, and applications to urban environmental problems. Int. J. Climatol. 31, 273–288. https://doi.org/10.1002/joc.2158.

Dixon, P.G., Mote, T.L., 2003. Patterns and causes of Atlanta's urban heat island–initiated precipitation. J. Appl. Meteorol. 42, 1273–1284. https://doi.org/10.1175/1520-0450(2003)042¡1273:pacoau¿2.0.co;2.
Doan, Q.V., Chen, F., Kusaka, H., Wang, J., Kajino, M., Takemi, T., 2022. Identifying a new normal in extreme precipitation at a city scale under warmer climate regimes: A case study of the Tokyo Metropolitan Area, Japan. J. Geophys. Res. Atmos. 127, e2022JD036810. URL: https://agupubs.onlinelibrary.wiley.com/doi/abs/10.1029/2022JD036810.
Doan, Q.V., Kobayashi, S., Kusaka, H., Chen, F., He, C., Niyogi, D., 2023. Tracking urban footprint on extreme precipitation in an African megacity. J. Appl. Meteorol. Climatol. 62, 209–226. URL: https://journals.ametsoc.org/view/journals/apme/62/2/JAMC-D-22-0048.1.xml https://doi.org/10.1175/JAMC-D-22-0048.1.
Donmez, B., Donmez, K., Diren-Ustun, D.H., Unal, Y., 2022. Urbanization-induced changes in convective and frontal precipitation events in Ankara. Urban Clim. 46, 101316. URL: https://www.sciencedirect.com/science/article/pii/S2212095522002346 https://doi.org/10.1016/j.uclim.2022.101316.
Dou, J., Wang, Y., Bornstein, R., Miao, S., 2015. Observed spatial characteristics of Beijing urban climate impacts on summer thunderstorms. J. Appl. Meteorol. Climatol. 54, 94–105. https://doi.org/10.1175/jamc-d-13-0355.1.
Dudhia, J., 1989. Numerical study of convection observed during the winter monsoon experiment using a mesoscale two-dimensional model. J. Atmos. Sci. 46, 3077–3107. https://doi.org/10.1175/1520-0469(1989)046¡3077:nsocod¿2.0.co;2.
Eliasson, I., Svensson, M.K., 2003. Spatial air temperature variations and urban land use — a statistical approach. Meteorol. Appl. 10, 135–149. https://doi.org/10.1017/s1350482703002056.
Feili, W., Shuangcheng, L., Dahai, L., Ze, L., Yongxun, W., Huan, W., Yueyao, W., Yajuan, Z., Yinglu, L., 2023. Analysis of the driving factors of precipitation change during the development of the jing-jin-ji urban agglomeration. Urban Clim. 51, 101613. URL: https://www.sciencedirect.com/science/article/pii/S2212095523002079 https://doi.org/10.1016/j.uclim.2023.101613.
Foissard, X., Dubreuil, V., Quénol, H., 2019. Defining scales of the land use effect to map the urban heat island in a mid-size European city: Rennes (France). Urban Clim. 29, 100490 https://doi.org/10.1016/j.uclim.2019.100490.
Gabriele, M., Simone, F., Elie, B.Z., Gabriel, G.K., 2020. Seasonal hysteresis of surface urban heat islands. Environ. Sci. 117, 7082–7089. https://doi.org/10.1073/pnas.1917554117.
Givati, A., Rosenfeld, D., 2004. Quantifying precipitation suppression due to air pollution. J. Appl. Meteorol. 43, 1038–1056. https://doi.org/10.1175/1520-0450(2004)043¡1038:qpsdta¿2.0.co;2.
Grillo, J.N., Spar, J., 1971. Rain-snow mesoclimatology of the New York metropolitan area. J. Appl. Meteorol. 10, 56–61. https://doi.org/10.1175/1520-0450(1971)010¡0056:rsmotn¿2.0.co;2.
Grimm, N.B., Faeth, S.H., Golubiewski, N.E., Redman, C.L., Wu, J., Bai, X., Briggs, J.M., 2008. Global change and the ecology of cities. Science 319, 756–760. https://doi.org/10.1126/science.1150195.
Guo, L., Fu, D., Wang, Y., Miao, S., 2019. A numerical study of urbanization impacts on a snowfall event in Beijing area. Acta. Meteor. Sin. 77, 835–848.
Hayhoe, K., VanDorn, J., Croley, T., Schlegal, N., Wuebbles, D., 2010. Regional climate change projections for Chicago and the US Great Lakes. J. Great Lakes Res. 36, 7–21. https://doi.org/10.1016/j.jglr.2010.03.012.
Hersbach, H., Bell, B., Berrisford, P., Biavati, G., Horányi, A., Muñoz Sabater, J., Nicolas, J., Peubey, C., Radu, R., Rozum, I., Schepers, D., Simmons, A., Soci, C., Dee, D., Thépaut, J.N., 2018. Era5 hourly data on single levels from 1959 to present. URL: 10.24381/cds.adbb2d47.
Hinkel, K.M., Nelson, F.E., 2007. Anthropogenic heat island at Barrow, Alaska, during winter: 2001–2005. J. Geophys. Res. Atmos. 1984–2012, 112. https://doi.org/10.1029/2006jd007837.
Hong, S.Y., Lim, K.S., Kim, J.H., Lim, J.O., 2006. The WRF single-moment-microphysics scheme class 6 (WSM6). Asia-Pac. J. Atmos. Sci. 42, 129–151.
Janjić, Z.I., 1994. The step-mountain eta coordinate model: further developments of the convection, viscous sublayer, and turbulence closure schemes. Mon. Weather Rev. 122, 927–945. https://doi.org/10.1175/1520-0493(1994)122¡0927:tsmecm¿2.0.co;2.
Johnson, B., Shepherd, J.M., 2018. An urban-based climatology of winter precipitation in the Northeast United States. Urban Clim. 24, 205–220. https://doi.org/10.1016/j.uclim.2018.03.003.
Johnson, B.D., Williams, M.D., Shepherd, J.M., 2021. Urbanization and winter precipitation: a case study analysis of land surface sensitivity. Atmosphere 12, 805. https://doi.org/10.3390/atmos12070805.
Jones, P.A., Jiusto, J.E., 1980. Some local climate trends in four cities of New York state. J. Appl. Meteorol. 19, 135–141. https://doi.org/10.1175/1520-0450(1980)019¡0135:slctif¿2.0.co;2.
Kim, Y.H., Baik, J.J., 2005. Spatial and temporal structure of the urban heat island in Seoul. J. Appl. Meteorol. 44, 591–605. https://doi.org/10.1175/jam2226.1.
Kim, G., Cha, D.H., Song, C.K., Kim, H., 2021. Impacts of anthropogenic heat and building height on urban precipitation over the Seoul metropolitan area in regional climate modeling. J. Geophys. Res. Atmos. 126, e2021JD035348. URL: https://agupubs.onlinelibrary.wiley.com/doi/abs/10.1029/2021JD035348.
Kitagawa, Y.K.L., de Almeida Albuquerque, T.T., Kumar, P., Nascimento, E.G.S., Moreira, D.M., 2022. Coastal-urban meteorology: a sensitivity study using the wrf-urban model. Urban Clim. 44, 101185. URL: https://www.sciencedirect.com/science/article/pii/S2212095522001031 https://doi.org/10.1016/j.uclim.2022.101185.
Li, D., Bou-Zeid, E., Baeck, M.L., Jessup, S., Smith, J.A., 2013. Modeling land surface processes and heavy rainfall in urban environments: sensitivity to urban surface representations. J. Hydrometeorol. 14, 130313080947004 https://doi.org/10.1175/jhm-d-12-0154.1.
Li, D., Malyshev, S., Shevliakova, E., 2016. Exploring historical and future URBAN climate in the Earth system modeling framework: 2. Impact of urban land use over the continental United States: URBAN CLIMATE IN EARTH SYSTEM MODELS. J. Adv. Model. Earth Syst. 8, 936–953. https://doi.org/10.1002/2015ms000579.
Liu, J., Niyogi, D., 2019. Meta-analysis of urbanization impact on rainfall modification. Sci. Rep. 9, 7301. https://doi.org/10.1038/s41598-019-42494-2.
Louis, M., Gunnar, M., Birthe, M.S., Øivind, H., Kari, A., Jana, S., 2020. Urbanization in megacities increases the frequency of extreme precipitation events far more than their intensity. Environ. Res. Lett. 15, 124072. URL: https://doi.org/10.1088/1748-9326/abcc8f https://doi.org/10.1088/1748-9326/abcc8f.
Makarieva, A.M., Gorshkov, V.G., Li, B.L., 2009. Precipitation on land versus distance from the ocean: evidence for a forest pump of atmospheric moisture. Ecol. Complex. 6, 302–307. https://doi.org/10.1016/j.ecocom.2008.11.004.
Malevich, S.B., Klink, K., 2011. Relationships between snow and the wintertime Minneapolis urban heat island. J. Appl. Meteorol. Climatol. 50, 1884–1894. https://doi.org/10.1175/jamc-d-11-05.1.
Menne, M.J., Durre, I., Vose, R.S., Gleason, B.E., Houston, T.G., 2012. An overview of the global historical climatology network-daily database. J. Atmos. Ocean. Technol. 29, 897–910. https://doi.org/10.1175/jtech-d-11-00103.1.
Miao, S., Chen, F., LeMone, M.A., Tewari, M., Li, Q., Wang, Y., 2009. An observational and modeling study of characteristics of urban heat island and boundary layer structures in Beijing. J. Appl. Meteorol. Climatol. 48, 484–501. https://doi.org/10.1175/2008jamc1909.1.
Miles, V., Esau, I., 2017. Seasonal and spatial characteristics of urban heat sslands (UHIs) in northern west Siberian cities. Remote Sens. 9, 989. https://doi.org/10.3390/rs9100989.
Mlawer, E.J., Taubman, S.J., Brown, P.D., Iacono, M.J., Clough, S.A., 1997. Radiative transfer for inhomogeneous atmospheres: RRTM, a validated correlated-k model for the longwave. J. Geophys. Res. Atmos. 102, 16663–16682. https://doi.org/10.1029/97jd00237.
Monin, A., Obukhov, S., 1954. Basic laws of turbulent mixing in the surface layer of the atmosphere. Contrib. Geophys. Inst. Acad. Sci. USSR 151, e187.
Montávez, J.P., Rodríguez, A., Jiménez, J.I., 2000. A study of the urban heat island of Granada. Int. J. Climatol. 20, 899–911. https://doi.org/10.1002/1097-0088(20000630)20:8¡899::aid-joc433¿3.0.co;2-i.
Niyogi, D., Holt, T., Zhong, S., Pyle, P.C., Basara, J., 2006. Urban and land surface effects on the 30 July 2003 mesoscale convective system event observed in the southern Great Plains. J. Geophys. Res. Atmos. 111 https://doi.org/10.1029/2005jd006746.
Niziol, T.A., Snyder, W.R., Waldstreicher, J.S., 1995. Winter weather forecasting throughout the eastern United States. Part IV: Lake effect snow. Weather Forecast. 10, 61–77. https://doi.org/10.1175/1520-0434(1995)010¡0061:wwftte¿2.0.co;2.
Notaro, M., Bennington, V., Vavrus, S., 2015. Dynamically downscaled projections of lake-effect snow in the Great Lakes basin. J. Clim. 28, 1661–1684. https://doi.org/10.1175/jcli-d-14-00467.1.

Ogino, S.Y., Yamanaka, M.D., Mori, S., Matsumoto, J., 2016. How much is the precipitation amount over the tropical coastal region? J. Clim. 29, 1231–1236. https://doi.org/10.1175/jcli-d-15-0484.1.
Oke, T.R., Mills, G., Christen, A., Voogt, J.A., 2017. Urban climates. Cambridge University Press. https://doi.org/10.1017/9781139016476.003.
Pauleit, S., Ennos, R., Golding, Y., 2005. Modeling the environmental impacts of urban land use and land cover change—a study in Merseyside, UK. Landsc. Urban Plan. 71, 295–310. https://doi.org/10.1016/j.landurbplan.2004.03.009.
Pielke, R.A., Adegoke, J., Beltrán-Przekurat, A., Hiemstra, C.A., Lin, J., Nair, U.S., Niyogi, D., Nobis, T.E., 2007. An overview of regional land-use and land-cover impacts on rainfall. Tellus B 59, 587–601. https://doi.org/10.1111/j.1600-0889.2007.00251.x.
Pielke, R.A., Pitman, A., Niyogi, D., Mahmood, R., McAlpine, C., Hossain, F., Goldewijk, K.K., Nair, U., Betts, R., Fall, S., Reichstein, M., Kabat, P., Noblet, N.D., 2011. Land use/land cover changes and climate: modeling analysis and observational evidence. Wiley Interdiscip. Rev. Clim. Chang. 2, 828–850. https://doi.org/10.1002/wcc.144.
Ramamurthy, P., Sangobanwo, M., 2016. Inter-annual variability in urban heat island intensity over 10 major cities in the United States. Sustain. Cities Soc. 26, 65–75. https://doi.org/10.1016/j.scs.2016.05.012.
Rosenfeld, D., 2000. Suppression of rain and snow by urban and industrial air pollution. Science 287, 1793–1796. https://doi.org/10.1126/science.287.5459.1793.
Ryu, Y.H., Smith, J.A., Bou-Zeid, E., Baeck, M.L., 2016. The influence of land surface heterogeneities on heavy convective rainfall in the Baltimore–Washington metropolitan area. Mon. Weather Rev. 144, 553–573. https://doi.org/10.1175/mwr-d-15-0192.1.
Sati, A.P., Mohan, M., 2021. Impact of urban sprawls on thunderstorm episodes: assessment using wrf model over central-national capital region of India. Urban Clim. 37, 100869. URL: https://www.sciencedirect.com/science/article/pii/S2212095521000997 https://doi.org/10.1016/j.uclim.2021.100869.
Shepherd, J.M., 2005. A review of current investigations of urban-induced rainfall and recommendations for the future. Earth Interact. 9, 1–27. https://doi.org/10.1175/ei156.1.
Shepherd, M., 2013. Impacts of urbanization on precipitation and storms: physical insights and vulnerabilities. Clim. Vulner. 5, 109–125.
Shu, C., Gaur, A., Wang, L., Lacasse, M.A., 2023. Evolution of the local climate in Montreal and Ottawa before, during and after a heatwave and the effects on urban heat islands. Sci. Total Environ. 890, 164497. URL: https://www.sciencedirect.com/science/article/pii/S0048969723031182 https://doi.org/10.1016/j.scitotenv.2023.164497.
Skamarock, W.C., Klemp, J.B., Dudhia, J., Gill, D.O., Powers, J.G., 2008. A description of the advanced research WRF version 3. In: Technical Report. NCAR Technical Note, Mesoscale and Microscale Meteorology Division. National Center for Atmospheric Research, Boulder, Colorado, USA.
Stensrud, D.J., 2007. Parameterization schemes: Keys to under-standing numerical weather prediction models. CambridgeUniversity Press.
Suomi, J., Hjort, J., Käyhkö, J., 2012. Effects of scale on modelling the urban heat island in Turku, SW Finland. Clim. Res. 55, 105–118. https://doi.org/10.3354/cr01123.
Taichen, F., Tiangang, Y., Jiahui, C., Zhikuan, W., Rong, Z., Zhiyuan, H., Jianping, H., 2023. The influence of dust on extreme precipitation at a large city in North China. Sci. Total Environ. 901, 165890. URL: https://www.sciencedirect.com/science/article/pii/S0048969723045151 https://doi.org/10.1016/j.scitotenv.2023.165890.
Thériault, J.M., Stewart, R.E., Henson, W., 2010. On the dependence of winter precipitation types on temperature, precipitation rate, and associated features. J. Appl. Meteorol. Climatol. 49, 1429–1442. https://doi.org/10.1175/2010jamc2321.1.
Wang, X., Wang, Z., Qi, Y., Guo, H., 2009. Effect of urbanization on the winter precipitation distribution in Beijing area. Sci. China Ser. D Earth Sci. 52, 250–256. https://doi.org/10.1007/s11430-009-0019-x.
WBGU, 2016. The Urban Planet: How Cities Save our Future. URL: https://www.environmentandsociety.org/mml.
Yang, J., Bou-Zeid, E., 2018. Should cities embrace their heat islands as shields from extreme cold? J. Appl. Meteorol. Climatol. 57, 1309–1320. https://doi.org/10.1175/jamc-d-17-0265.1.
Yang, C., Tao, Z.Y., Ze-Chun, L.I., 2009. Overview of research on ocean (lake)-effect snow. Mar. Sci. Bull. 28, 81–88.
Yang, L., Smith, J.A., Baeck, M.L., Bou-Zeid, E., Jessup, S.M., Tian, F., Hu, H., 2014a. Impact of urbanization on heavy convective precipitation under strong large-scale forcing: A case study over the Milwaukee–Lake Michigan region. J. Hydrometeorol. 15, 261–278. https://doi.org/10.1175/jhm-d-13-020.1.
Yang, L., Tian, F., Smith, J.A., Hu, H., 2014b. Urban signatures in the spatial clustering of summer heavy rainfall events over the Beijing metropolitan region. J. Geophys. Res. Atmos. 119, 1203–1217. https://doi.org/10.1002/2013jd020762.
Yang, L., Smith, J., Niyogi, D., 2019. Urban impacts on extreme monsoon rainfall and flooding in complex terrain. Geophys. Res. Lett. 46, 5918–5927. https://doi.org/10.1029/2019gl083363.
Yang, L., Ni, G., Tian, F., Niyogi, D., 2021. Urbanization exacerbated rainfall over European suburbs under a warming climate. Geophys. Res. Lett. 48 https://doi.org/10.1029/2021gl095987.
Zhang, W., Villarini, G., Vecchi, G.A., Smith, J.A., 2018. Urbanization exacerbated the rainfall and flooding caused by hurricane Harvey in Houston. Nature 563, 384–388. https://doi.org/10.1038/s41586-018-0676-z.
Zhao, C., Fu, G., Liu, X., Fu, F., 2011. Urban planning indicators, morphology and climate indicators: a case study for a north-south transect of Beijing, China. Build. Environ. 46, 1174–1183. https://doi.org/10.1016/j.buildenv.2010.12.009.
Zhong, S., Qian, Y., Zhao, C., Leung, R., Wang, H., Yang, B., Fan, J., Yan, H., Yang, X.Q., Liu, D., 2017. Urbanization-induced urban heat island and aerosol effects on climate extremes in the Yangtze River Delta region of China. Atmos. Chem. Phys. 17, 5439–5457. https://doi.org/10.5194/acp-17-5439-2017.
Zhou, D., Zhang, L., Li, D., Huang, D., Zhu, C., 2016. Climate–vegetation control on the diurnal and seasonal variations of surface urban heat islands in China. Environ. Res. Lett. 11, 074009 https://doi.org/10.1088/1748-9326/11/7/074009.